

Computational Science Laboratory Technical Report CSL-TR-18 -2 September 5, 2018

Mahesh Narayanamurthi, Paul Tranquilli, Adrian
Sandu and Mayya Tokman

“EPIRK- W and EPIRK- K time discretization
methods”

Computational Science Laboratory
Computer Science Department
Virginia Polytechnic Institute and State University
Blacksburg, VA 24060
Phone: (540)-231-2193
Fax: (540)-231-6075
Email: maheshnm@vt.edu
Web: <http://csl.cs.vt.edu>



EPIRK- W and EPIRK- K time discretization methods

Mahesh Narayanamurthi^a, Paul Tranquilli^a, Adrian Sandu^a, Mayya Tokman^b

^a*Computational Science Laboratory, Department of Computer Science, Virginia Tech, Blacksburg, VA 24060*

^b*School of Natural Sciences, University of California, Merced, CA 95343*

Abstract

Exponential integrators are special time discretization methods where the traditional linear system solves used by implicit schemes are replaced with computing the action of matrix exponential-like functions on a vector. A very general formulation of exponential integrators is offered by the Exponential Propagation Iterative methods of Runge-Kutta type (EPIRK) family of schemes. The use of Jacobian approximations is an important strategy to drastically reduce the overall computational costs of implicit schemes while maintaining the quality of their solutions. This paper extends the EPIRK class to allow the use of inexact Jacobians as arguments of the matrix exponential-like functions. Specifically, we develop two new families of methods: EPIRK- W integrators that can accommodate any approximation of the Jacobian, and EPIRK- K integrators that rely on a specific Krylov-subspace projection of the exact Jacobian. Classical order conditions theories are constructed for these families. A practical EPIRK- W method of order three and an EPIRK- K method of order four are developed. Numerical experiments indicate that the methods proposed herein are computationally favorable when compared to existing exponential integrators.

Contents

1	Introduction	2
2	Exponential Propagation Iterative methods of Runge-Kutta type	3
3	EPIRK-W methods	4
3.1	Order conditions theory for EPIRK- W methods	5
3.2	Construction of practical EPIRK- W integrators	14
4	EPIRK-K methods	15
4.1	Krylov-subspace approximation of Jacobian	16
4.2	Formulation of EPIRK- K methods	17
4.3	Order conditions theory for EPIRK- K methods	18
4.4	Construction of practical EPIRK- K integrators	21
5	Implementation strategies for exponential integrators	22
6	Numerical results	23
6.1	Lorenz-96 system	24
6.2	Shallow water equations on the sphere	28
6.3	The Allen-Cahn problem	31

Email addresses: maheshnm@vt.edu (Mahesh Narayanamurthi), ptranq@vt.edu (Paul Tranquilli), sandu@cs.vt.edu (Adrian Sandu), mtokman@ucmerced.edu (Mayya Tokman)

7	Conclusions	36
A	Derivation of K-methods	36
B	Proofs	39
C	Structure of Jacobian evaluated at y_0 for the test problems	42

1. Introduction

The following initial value problem for a system of ordinary differential equations (ODEs)

$$y' = f(t, y), \quad y(t_0) = y_0, \quad t_0 \leq t \leq t_F, \quad y(t) \in \mathbb{R}^N. \quad (1)$$

arises in many applications including numerical solution of partial differential equations (PDEs) using a method of lines. Different time discretization methods can then be applied to solve (1) and approximate numerical solutions $y_n \approx y(t_n)$ at discrete times t_n .

Runge-Kutta methods [6] are the prototypical one-step discretizations that use internal stage approximations to propagate the numerical solution forward in time from t_n to $t_{n+1} = t_n + h$. Explicit Runge-Kutta methods [6, Section II.2] perform inexpensive calculations at each step, but suffer from stability restrictions on the time step size which makes them inappropriate for solving stiff systems. Implicit Runge-Kutta methods [6, Section II.7] require solution of non-linear systems of equations at each step that can be done, for instance, by using a Newton-like approach. This eases the numerical stability restrictions and allows to use large time step sizes for stiff problems, however it also increases the computational cost per step.

Rosenbrock methods [7, Section IV.7] arise from linearization of diagonally implicit Runge-Kutta methods, and solve only linear systems of equations at each time step. The Jacobian of the ODE function (1)

$$\mathbf{J}(t, y) = \frac{\partial f(t, y)}{\partial y} \quad (2)$$

appears explicitly in the formulation of the method, and the order conditions theory relies on using an exact Jacobian during computations. For the solution of large linear systems a popular implementation uses Krylov projection-based iterative methods such as GMRES. Early truncation of the iterative method is equivalent to the use of an approximation of the Jacobian, and the overall scheme may suffer from order reduction [24]. Rosenbrock-W (ROW) methods [7, Section IV.7] mitigate this by admitting arbitrary approximations of the Jacobian ($\mathbf{A} \approx \mathbf{J}$). This is possible at the cost of a vastly increased number of order conditions, and by using many more stages to allow for enough degrees of freedom to satisfy them. Rosenbrock-K (ROK) methods [26] are built in the ROW framework by making use of a specific Krylov-based approximation of the Jacobian. This approximation leads to a number of trees that arise in ROW order conditions theory to become isomorphic to one another, leading to a dramatic reduction in the total number of order conditions.

Exponential integrators [8, 10, 17, 20, 21] are a class of timestepping methods that replace the linear system solves in Rosenbrock style methods with operations involving the action of matrix exponential-like functions on a vector. For many problems these products of a matrix exponential-like function with a vector can be evaluated more efficiently than solving the corresponding linear systems.

Both the W -versions [9] and K -versions [25] of exponential methods have been established for particular formulations of exponential methods. This paper extends the theory of W - and K -type methods to the general class of Exponential Propagation Iterative methods of Runge-Kutta type (EPIRK) [20, 21].

The remainder of the paper is laid out as follows. In Section 2, we describe the general form of the EPIRK method and some simplifying assumptions that we make in this paper. In Section 3, we derive the order conditions for an EPIRK- W method and construct methods with two different sets of coefficients. In Section 4, we extend the K -theory to EPIRK method and construct an EPIRK- K method. Section 5 addresses strategies to evaluate products involving exponential like functions of matrices and vectors that are present in the formulation of methods discussed in this paper. Section 6 presents the numerical results, and conclusions are drawn in Section 7.

2. Exponential Propagation Iterative methods of Runge-Kutta type

A very general formulation of exponential integrators is offered by the EPIRK family of methods, which was first introduced in [20]. As is typical for exponential methods, the formulation of EPIRK is derived from the following integral form of the problem (1) on the time interval $[t_n, t_n + h]$:

$$y(t_n + h) = y_n + h \varphi_1(h \mathbf{J}_n) f(y_n) + h \int_0^1 e^{h \mathbf{J}_n (1-\theta)} r(y(t_n + \theta h)) d\theta. \quad (3)$$

Equation (3) is derived by splitting the right hand-side function of (1) into a linear term and non-linear remainder using first-order Taylor expansion

$$y' = f(y_n) + \mathbf{J}_n (y - y_n) + r(y), \quad r(y) := f(y) - f(y_n) - \mathbf{J}_n (y - y_n), \quad (4)$$

and using the integrating factor method to transform this ODE into an integral equation [21]. In equation (3) the Jacobian matrix (2) evaluated at time t_n is $\mathbf{J}_n = \mathbf{J}(t_n, y_n)$, and $r(y)$ is the non-linear remainder term of the Taylor expansion of the right-hand side function. The function $\varphi_1(z) = (e^z - 1)/z$ is the first one in the sequence of analytic functions defined by

$$\varphi_k(z) = \int_0^1 e^{z(1-\theta)} \frac{\theta^{k-1}}{(k-1)!} d\theta = \sum_{i=0}^{\infty} \frac{z^i}{(i+k)!}, \quad k = 1, 2, \dots, \quad (5)$$

and satisfying the recurrence relation

$$\varphi_0(z) = e^z; \quad \varphi_{k+1}(z) = \frac{\varphi_k(z) - 1/k!}{z}, \quad k = 1, 2, \dots; \quad \varphi_k(0) = \frac{1}{k!}. \quad (6)$$

As explained in [21], the construction of exponential numerical integrators requires to numerically approximate the integral term in equation (3), and to compute exponential-like matrix function times vector products $\varphi_k(\cdot) v$ that include the second term in the right hand side of (3) as well as additional terms needed by the integral approximation.

Construction of an EPIRK-type scheme begins by considering a general ansatz [21] that describes an s -stage method:

$$\begin{aligned} Y_i &= y_n + a_{i,1} \psi_{i,1}(g_{i,1} h \mathbf{A}_{i,1}) h f(y_n) + \sum_{j=2}^i a_{i,j} \psi_{i,j}(g_{i,j} h \mathbf{A}_{i,j}) h \Delta^{(j-1)} r(y_n), \quad i = 1, \dots, s-1, \\ y_{n+1} &= y_n + b_1 \psi_{s,1}(g_{s,1} h \mathbf{A}_{s,1}) h f(y_n) + \sum_{j=2}^s b_j \psi_{s,j}(g_{s,j} h \mathbf{A}_{s,j}) h \Delta^{(j-1)} r(y_n), \end{aligned} \quad (7)$$

where Y_i are the internal stage vectors; y_n , also denoted as Y_0 , is the input stage vector; and y_{n+1} is the final output stage of a single step. The j -th forward difference $\Delta^{(j)} r(y_n)$ is calculated using the residual values at the stage vectors:

$$\Delta^{(1)} r(Y_i) = r(Y_{i+1}) - r(Y_i), \quad \Delta^{(j)} r(Y_i) = \Delta^{(j-1)} r(Y_{i+1}) - \Delta^{(j-1)} r(Y_i).$$

Particular choices of matrices \mathbf{A}_{ij} , functions ψ_{ij} and $r(y)$ define classes of EPIRK methods as well as allow derivation of specific schemes. In this paper we will focus on general, so called unpartitioned, EPIRK methods which can be constructed from (7) by choosing all matrices as a Jacobian matrix evaluated at t_n , i.e. $\mathbf{A}_{ij} = \mathbf{J}_n$, function $r(y)$ to be the remainder of the first-order Taylor expansion of $f(y)$ as in (4) and functions ψ_{ij} to be linear combinations of φ_k 's:

$$\psi_{i,j}(z) = \sum_{k=1}^s p_{i,j,k} \varphi_k(z). \quad (8)$$

Here we will also use the simplifying assumption from [21, eq. 25]

$$\psi_{i,j}(z) = \psi_j(z) = \sum_{k=1}^j p_{j,k} \varphi_k(z). \quad (9)$$

These choices lead to the class of general unpartitioned EPIRK schemes described by

$$\begin{aligned} Y_i &= y_n + a_{i,1} \psi_1(g_{i,1} h \mathbf{J}_n) h f(y_n) + \sum_{j=2}^i a_{i,j} \psi_j(g_{i,j} h \mathbf{J}_n) h \Delta^{(j-1)} r(y_n), \quad i = 1, \dots, s-1, \\ y_{n+1} &= y_n + b_1 \psi_1(g_{s,1} h \mathbf{J}_n) h f(y_n) + \sum_{j=2}^s b_j \psi_j(g_{s,j} h \mathbf{J}_n) h \Delta^{(j-1)} r(y_n). \end{aligned} \quad (10)$$

Coefficients $p_{j,k}$, $a_{i,j}$, $g_{i,j}$, and b_j have to be determined from order conditions to build schemes of specific order.

Remark 2.1. *Computationally efficient strategies to evaluate exponential-like matrix function times vector products vary depending on the size of the ODE system. Approximating products $\psi(z)v$ constitutes the major portion of overall computational cost of the method. Taylor expansion or Pade based approximations can be used to evaluate the products $\psi(z)v$ for small systems. For large scale problems, particularly those where matrices cannot be stored explicitly and a matrix-free formulation of an integrator is a necessity, Krylov projection-based methods become the de facto choice [21].*

EPIRK methods of a given order can be built by solving either classical [21] or stiff [15] order conditions. In this paper we will focus on the classically accurate EPIRK methods. A classical EPIRK scheme is constructed by matching required number of Taylor expansion coefficients of the exact and approximate solutions to derive order conditions. The order conditions are then solved to compute the coefficients of the method. To ensure that the error has the desired order the exact Jacobian matrix \mathbf{J}_n has to be used in the Taylor expansion of the numerical solution. If the Jacobian or its action on a vector is not computed with full accuracy, the numerical method will suffer from order reduction.

In this paper we construct EPIRK methods that retain full accuracy even with an approximated Jacobian. The theory of using inexact Jacobians in the method formulation, first proposed in [19] for implicit schemes, is extended to EPIRK methods. More specifically, EPIRK- W methods that admit arbitrary approximations of the Jacobian while maintaining full order of accuracy are derived in Section 3. The drawback of W -methods, as mentioned in [7, section IV.7], is the very fast growth of the number of order conditions with increasing order of the method. In such cases, significantly larger number of stages are typically needed to build higher-order methods.

In [25, 26] we developed K -methods, versions of W -methods that use a specific Krylov-subspace approximation of the Jacobian, and dramatically reduce the number of necessary order conditions. Here we construct K -methods for EPIRK schemes in Section 4. The K -method theory enables the construction of high order methods with significantly fewer stages than W -methods. For example, we show that three stage EPIRK W -methods only exist up to order three, whereas we derive here a fourth order K -method. Furthermore, as shown in the numerical results in Section 6, for some problems K -methods have better computational performance than traditional exponential integrators.

3. EPIRK- W methods

An EPIRK- W method is formulated like a traditional EPIRK method (10) with the only difference being the use of an inexact Jacobian (\mathbf{A}_n) in place of the exact Jacobian (\mathbf{J}_n). Using the simplification (9) the

method reads:

$$\begin{aligned}
Y_i &= y_n + a_{i,1} \psi_1(g_{i,1} h \mathbf{A}_n) h f(y_n) + \sum_{j=2}^i a_{i,j} \psi_j(g_{i,j} h \mathbf{A}_n) h \Delta^{(j-1)} r(y_n), \quad i = 1, \dots, s-1, \\
y_{n+1} &= y_n + b_1 \psi_1(g_{s,1} h \mathbf{A}_n) h f(y_n) + \sum_{j=2}^s b_j \psi_j(g_{s,j} h \mathbf{A}_n) h \Delta^{(j-1)} r(y_n).
\end{aligned} \tag{11}$$

This modification requires the order conditions theory to be modified to accommodate this approximation.

3.1. Order conditions theory for EPIRK-W methods

The classical order conditions for EPIRK-W methods result from matching the Taylor series expansion coefficients of the numerical solution y_{n+1} up to a certain order with those from the Taylor series expansion of the exact solution $y(t_n + h)$. The construction of order conditions is conveniently expressed in terms of Butcher trees [6]. The trees corresponding to the elementary differentials of the numerical solution are the *TW*-trees. *TW*-trees are rooted Butcher trees with two different colored nodes - fat (empty) and meagre (full) - such that the end vertices are meagre and the fat vertices are singly branched. The *TW*-trees up to order four are shown in Tables 1 and 2 following [25].

In *TW*-trees that correspond to elementary differentials of the Taylor expansion of numerical solution, the meagre nodes represents the appearance of f and its derivatives. The fat nodes represent the appearance of the inexact Jacobian \mathbf{A}_n . It is useful to note that trees that contain both meagre and fat nodes do not appear in the trees corresponding to the Taylor expansion of the exact solution, as such an expansion does not contain the inexact Jacobian.

In order to construct the order conditions for the *W*-method we rely on B-series theory. A B-series [6, Section II.12] is an operator that maps a set of trees onto the set of real coefficients corresponding to the coefficients of the elementary differentials in a Taylor expansion. If $\mathbf{a} : TW \cup \emptyset \rightarrow \mathbb{R}$ is a mapping from the set of *TW* trees and the empty tree to real numbers the corresponding B-series is given by:

$$B(\mathbf{a}, y) = \mathbf{a}(\emptyset) y + \sum_{\tau \in TW} \mathbf{a}(\tau) \frac{h^{|\tau|}}{\sigma(\tau)} F(\tau)(y).$$

Here τ is a *TW*-tree and $|\tau|$ is the order of the tree (the number of nodes of the *TW*-tree), and $\sigma(\tau)$ is the order of the symmetry group of the tree [3, 21]. A simple algorithm for evaluating $\sigma(\tau)$ is given in [21]. Lastly, $F(\tau)(y)$ maps a tree to the corresponding elementary differential.

We also make use of the operator $B^\#(g)$, first defined in [25], which takes a B-series g and returns its coefficients. Therefore:

$$B^\#(B(\mathbf{a}, y)) = \mathbf{a}.$$

Tables 1 and 2 list both *TW*- and *TK*-trees up to order four and the corresponding tree names. *TK*-trees which are a subset of *TW*-trees will be central to the discussion of *K*-methods in the next section. The subsequent rows of the two tables show the following:

- The elementary differentials corresponding to each *TW*-trees up to order four.
- A set of coefficients x_i for an arbitrary B-series $\mathbf{a}(\tau)$.
- The coefficients of the B-series resulting from composing the function f with the B-series $\mathbf{a}(\tau)$. The rules for composing B-series are discussed in [4, 21].
- The coefficients of the B-series resulting from left-multiplying the B-series $\mathbf{a}(\tau)$ by an inexact Jacobian. The multiplication rule for B-series is explained in [4].




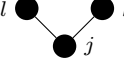
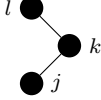
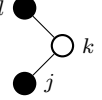
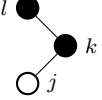
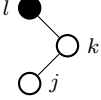
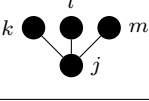
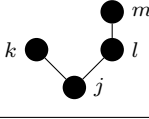
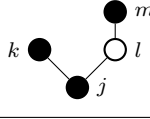
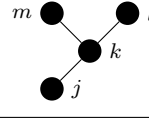
τ				
W-tree name	τ_1^W	τ_2^W	τ_3^W	τ_4^W
K-tree name	τ_1^K	τ_2^K	—	τ_3^K
$F(\tau)$	f^J	$f_K^J f^K$	$\mathbf{A}_{JK} f^K$	$f_{KL}^J f^K f^L$
$\mathbf{a}(\tau)$	x_1	x_2	x_3	x_4
$B^\#(hf(B(\mathbf{a}, y)))$	1	x_1	0	x_1^2
$B^\#(h\mathbf{A}B(\mathbf{a}, y))$	0	0	x_1	0
$B^\#(\varphi_j(h\mathbf{A})B(\mathbf{a}, y))$	$c_0 x_1$	$c_0 x_2$	$c_0 x_3 + c_1 x_1$	$c_0 x_4$
τ				
W-tree name	τ_5^W	τ_6^W	τ_7^W	τ_8^W
K-tree name	τ_4^K	—	—	—
$F(\tau)$	$f_K^J f_L^K f^L$	$f_K^J \mathbf{A}_{KL} f^L$	$\mathbf{A}_{JK} f_L^K f^L$	$\mathbf{A}_{JK} \mathbf{A}_{KL} f^L$
$\mathbf{a}(\tau)$	x_5	x_6	x_7	x_8
$B^\#(hf(B(\mathbf{a}, y)))$	x_2	x_3	0	0
$B^\#(h\mathbf{A}B(\mathbf{a}, y))$	0	0	x_2	x_3
$B^\#(\varphi_j(h\mathbf{A})B(\mathbf{a}, y))$	$c_0 x_5$	$c_0 x_6$	$c_0 x_7 + c_1 x_2$	$c_0 x_8 + c_1 x_3 + c_2 x_1$
τ				
W-tree name	τ_9^W	τ_{10}^W	τ_{11}^W	τ_{12}^W
K-tree name	τ_5^K	τ_6^K	—	τ_7^K
$F(\tau)$	$f_{KLM}^J f^K f^L f^M$	$f_{KL}^J f_M^L f^M f^K$	$f_{KL}^J \mathbf{A}_{LM} f^M f^K$	$f_K^J f_{LM}^K f^M f^L$
$\mathbf{a}(\tau)$	x_9	x_{10}	x_{11}	x_{12}
$B^\#(hf(B(\mathbf{a}, y)))$	x_1^3	$x_1 x_2$	$x_1 x_3$	x_4
$B^\#(h\mathbf{A}B(\mathbf{a}, y))$	0	0	0	0
$B^\#(\varphi_j(h\mathbf{A})B(\mathbf{a}, y))$	$c_0 x_9$	$c_0 x_{10}$	$c_0 x_{11}$	$c_0 x_{12}$

Table 1: TW-trees up to order four (part one of two).

- The coefficients of the B-series resulting from left-multiplying the B-series $\mathbf{a}(\tau)$ by $\varphi_j(h\mathbf{A}_n)$. The rules for multiplying a B-series by $\psi(h\mathbf{J}_n)$, where \mathbf{J}_n is the exact Jacobian at y_n , are given in [21]. The rules for multiplying a B-series by $\psi(h\mathbf{A}_n)$, for an arbitrary matrix \mathbf{A}_n , are given in [25].

In addition, we note that the B and $B^\#$ operators are linear. Consequently, the B-series of the sum of two arbitrary functions is the sum of the B-series of each and likewise, the operator $B^\#$ returns the sum of the coefficients of each lined up against corresponding elementary differentials.

Using B-series operations, as described above, one can systematically construct the B-series coefficients of the EPIRK- W numerical solution. This is achieved in Algorithm 1. The algorithm starts by initializing the set of B-series coefficients to those of the solution at the current time step, y_n . Next, the algorithm operates on the sequence of coefficients by applying the B-series operations that correspond to the mathematical

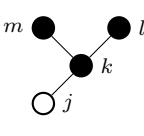
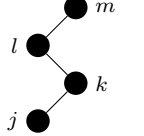
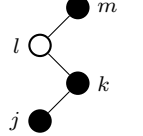
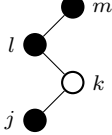
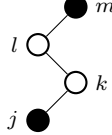
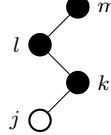
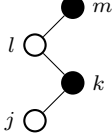
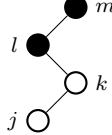
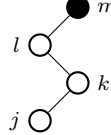
τ			
W-tree name	τ_{13}^W	τ_{14}^W	τ_{15}^W
K-tree name	τ_8^K	τ_9^K	—
$F(\tau)$	$\mathbf{A}_{JK} f_{LM}^K f^L f^M$	$f_K^J f_L^K f_M^L f^M$	$f_K^J f_L^K \mathbf{A}_{LM} f^M$
$\mathbf{a}(\tau)$	x_{13}	x_{14}	x_{15}
$B^\#(hf(B(\mathbf{a}, y)))$	0	x_5	x_6
$B^\#(h\mathbf{A}B(\mathbf{a}, y))$	x_4	0	0
$B^\#(\varphi_j(h\mathbf{A})B(\mathbf{a}, y))$	$c_0 x_{13} + c_1 x_4$	$c_0 x_{14}$	$c_0 x_{15}$
τ			
W-tree name	τ_{16}^W	τ_{17}^W	τ_{18}^W
K-tree name	—	—	—
$F(\tau)$	$f_K^J \mathbf{A}_{KL} f_M^L f^M$	$f_K^J \mathbf{A}_{KL} \mathbf{A}_{LM} f^M$	$\mathbf{A}_{JK} f_L^K f_M^L f^M$
$\mathbf{a}(\tau)$	x_{16}	x_{17}	x_{18}
$B^\#(hf(B(\mathbf{a}, y)))$	x_7	x_8	0
$B^\#(h\mathbf{A}B(\mathbf{a}, y))$	0	0	x_5
$B^\#(\varphi_j(h\mathbf{A})B(\mathbf{a}, y))$	$c_0 x_{16}$	$c_0 x_{17}$	$c_0 x_{18} + c_1 x_5$
τ			
W-tree name	τ_{19}^W	τ_{20}^W	$\tau_{2,1}^W$
K-tree name	—	—	—
$F(\tau)$	$\mathbf{A}_{JK} f_L^K \mathbf{A}_{LM} f^M$	$\mathbf{A}_{JK} \mathbf{A}_{KL} f_M^L f^M$	$\mathbf{A}_{JK} \mathbf{A}_{KL} \mathbf{A}_{LM} f^M$
$\mathbf{a}(\tau)$	x_{19}	x_{20}	x_{21}
$B^\#(hf(B(\mathbf{a}, y)))$	0	0	0
$B^\#(h\mathbf{A}B(\mathbf{a}, y))$	x_6	x_7	x_8
$B^\#(\varphi_j(h\mathbf{A})B(\mathbf{a}, y))$	$c_0 x_{19} + c_1 x_6$	$c_0 x_{20} + c_1 x_7 + c_2 x_2$	$c_0 x_{21} + c_1 x_8 + c_2 x_3 + c_3 x_1$

Table 2: TW-trees up to order four (part two of two).

calculations performed during each stage of the EPIRK- W method. All B-series operations are done on coefficient sets truncated to the desired order (order four herein). We repeat this process for each internal stage, and finally for the last stage, to obtain the coefficients of the B-series corresponding to the numerical solution of one EPIRK- W step.

We recall the following definition:

Algorithm 1 Compute the B-series coefficient of numerical solution

```

1: Input:  $y_n$  ▷ B-series coefficient of the current numerical solution.
2: for  $i = 1 : s - 1$  do ▷ Do for each internal stage of the method
3:    $u = B^\#(h f(B(y_n, y)))$  ▷ Composition of  $f$  with B-series of the current solution.
4:    $u = B^\#(\psi_{i,1}(h g_{i,1} \mathbf{A}_n) \cdot B(u, y))$  ▷ Multiplication by  $\psi$  function
5:    $u = a_{i,1} * u$  ▷ Scaling by a constant
6:   for  $j = 2 : i$  do
7:      $v = B^\#(h \Delta^{(j-1)} r(y_n))$  ▷ Recursive forward-difference
8:      $v = B^\#(\psi_{i,j}(h g_{i,j} \mathbf{A}_n) \cdot B(v, y))$ 
9:      $u = u + a_{i,j} * v$ 
10:  end for
11:   $Y_i = y_n + u$  ▷ Addition of two B-series
12: end for
13:  $u = B^\#(h f(B(y_n, y)))$ 
14:  $u = B^\#(\psi_{s,1}(h g_{s,1} \mathbf{A}_n) \cdot B(u, y))$ 
15:  $u = b_1 * u$ 
16: for  $j = 2 : s$  do
17:    $v = B^\#(h \Delta^{(j-1)} r(y_n))$ 
18:    $v = B^\#(\psi_{s,j}(h g_{s,j} \mathbf{A}_n) \cdot B(v, y))$ 
19:    $u = u + b_j * v$ 
20: end for
21:  $y_{n+1} = y_n + u$ 
22: Output:  $y_{n+1}$  ▷ B-series coefficient of the next step numerical solution.

```

Definition 3.1 (Density of a tree [3, 6]). *The density $\gamma(\tau)$ of a tree τ is the product over all vertices of the orders of the sub-trees rooted at those vertices.*

We have the following theorem.

Theorem 3.2 (B-series of the exact solution). *The B-series expansion of the exact solution at the next step $y(t_n + h)$, performed over TW-trees, has the following coefficients:*

$$a(\tau) = \begin{cases} 0 & \tau \in TW \setminus T, \\ \gamma(\tau) & \tau \in T. \end{cases}$$

Proof. First part of the proof follows from the observation that the elementary differentials in the B-series expansion of the exact solution cannot have the approximate Jacobian appearing anywhere in their expressions. Second part of the proof follows from [6, Theorem 2.6, 2.11] and [3, Subsection 302, 380]. \square

The EPIRK- W order conditions are obtained by imposing that the B-series coefficients of the numerical solution match the B-series coefficients of the exact solution up to the desired order of accuracy. The order conditions for the three stages EPIRK- W method (12) are given in Table 3.

Table 3: Order conditions for the three stage EPIRK- W method

Tree	Order	Order Condition: $B^\#(y_{n+1}) - B^\#(y(t_n + h)) = 0$
τ_1^W	1	$b_1 p_{1,1} - 1 = 0$

Tree	Order	Order Condition: $B^\#(y_{n+1}) - B^\#(y(t_n + h)) = 0$
τ_2^W	2	$\frac{1}{6}(6a_{1,1} b_2 p_{1,1} p_{2,1} + 3a_{1,1} b_2 p_{1,1} p_{2,2} - 12a_{1,1} b_3 p_{1,1} p_{3,1}$ $+ 6a_{2,1} b_3 p_{1,1} p_{3,1} - 6a_{1,1} b_3 p_{1,1} p_{3,2} + 3a_{2,1} b_3 p_{1,1} p_{3,2}$ $- 2a_{1,1} b_3 p_{1,1} p_{3,3} + a_{2,1} b_3 p_{1,1} p_{3,3} - 3) = 0$
τ_3^W	2	$\frac{1}{6}p_{1,1} (3b_1 g_{3,1} - 6a_{1,1} b_2 p_{2,1} - 3a_{1,1} b_2 p_{2,2}$ $+ 12a_{1,1} b_3 p_{3,1} - 6a_{2,1} b_3 p_{3,1} + 6a_{1,1} b_3 p_{3,2}$ $- 3a_{2,1} b_3 p_{3,2} + 2a_{1,1} b_3 p_{3,3} - a_{2,1} b_3 p_{3,3}) = 0$
τ_4^W	3	$\frac{1}{6} (6a_{1,1}^2 b_2 p_{2,1} p_{1,1}^2 + 3a_{1,1}^2 b_2 p_{2,2} p_{1,1}^2 - 12a_{1,1}^2 b_3 p_{3,1} p_{1,1}^2$ $+ 6a_{2,1}^2 b_3 p_{3,1} p_{1,1}^2 - 6a_{1,1}^2 b_3 p_{3,2} p_{1,1}^2 + 3a_{2,1}^2 b_3 p_{3,2} p_{1,1}^2$ $- 2a_{1,1}^2 b_3 p_{3,3} p_{1,1}^2 + a_{2,1}^2 b_3 p_{3,3} p_{1,1}^2 - 2) = 0$
τ_5^W	3	$\frac{1}{12} (12a_{1,1} a_{2,2} b_3 p_{1,1} p_{2,1} p_{3,1} + 6a_{1,1} a_{2,2} b_3 p_{1,1} p_{2,2} p_{3,1}$ $+ 6a_{1,1} a_{2,2} b_3 p_{1,1} p_{2,1} p_{3,2} + 3a_{1,1} a_{2,2} b_3 p_{1,1} p_{2,2} p_{3,2}$ $+ 2a_{1,1} a_{2,2} b_3 p_{1,1} p_{2,1} p_{3,3} + a_{1,1} a_{2,2} b_3 p_{1,1} p_{2,2} p_{3,3} - 2) = 0$
τ_6^W	3	$\frac{1}{12} p_{1,1} (6a_{1,1} b_2 g_{1,1} p_{2,1} - 12a_{1,1} a_{2,2} b_3 p_{3,1} p_{2,1}$ $- 6a_{1,1} a_{2,2} b_3 p_{3,2} p_{2,1} - 2a_{1,1} a_{2,2} b_3 p_{3,3} p_{2,1}$ $+ 3a_{1,1} b_2 g_{1,1} p_{2,2} - 12a_{1,1} b_3 g_{1,1} p_{3,1} + 6a_{2,1} b_3 g_{2,1} p_{3,1}$ $- 6a_{1,1} a_{2,2} b_3 p_{2,2} p_{3,1} - 6a_{1,1} b_3 g_{1,1} p_{3,2}$ $+ 3a_{2,1} b_3 g_{2,1} p_{3,2} - 3a_{1,1} a_{2,2} b_3 p_{2,2} p_{3,2} - 2a_{1,1} b_3 g_{1,1} p_{3,3}$ $+ a_{2,1} b_3 g_{2,1} p_{3,3} - a_{1,1} a_{2,2} b_3 p_{2,2} p_{3,3}) = 0$
τ_7^W	3	$\frac{1}{24} p_{1,1} (12a_{1,1} b_2 g_{3,2} p_{2,1} - 24a_{1,1} a_{2,2} b_3 p_{3,1} p_{2,1}$ $- 12a_{1,1} a_{2,2} b_3 p_{3,2} p_{2,1} - 4a_{1,1} a_{2,2} b_3 p_{3,3} p_{2,1}$ $+ 4a_{1,1} b_2 g_{3,2} p_{2,2} - 24a_{1,1} b_3 g_{3,3} p_{3,1} + 12a_{2,1} b_3 g_{3,3} p_{3,1}$ $- 12a_{1,1} a_{2,2} b_3 p_{2,2} p_{3,1} - 8a_{1,1} b_3 g_{3,3} p_{3,2}$ $+ 4a_{2,1} b_3 g_{3,3} p_{3,2} - 6a_{1,1} a_{2,2} b_3 p_{2,2} p_{3,2} - 2a_{1,1} b_3 g_{3,3} p_{3,3}$ $+ a_{2,1} b_3 g_{3,3} p_{3,3} - 2a_{1,1} a_{2,2} b_3 p_{2,2} p_{3,3}) = 0$

Tree	Order	Order Condition: $B^\#(y_{n+1}) - B^\#(y(t_n + h)) = 0$
τ_8^W	3	$\begin{aligned} & \frac{1}{24} p_{1,1} (4b_1 g_{3,1}^2 - 12a_{1,1} b_2 g_{1,1} p_{2,1} - 12a_{1,1} b_2 g_{3,2} p_{2,1} \\ & - 6a_{1,1} b_2 g_{1,1} p_{2,2} - 4a_{1,1} b_2 g_{3,2} p_{2,2} + 24a_{1,1} b_3 g_{1,1} p_{3,1} \\ & - 12a_{2,1} b_3 g_{2,1} p_{3,1} + 24a_{1,1} b_3 g_{3,3} p_{3,1} - 12a_{2,1} b_3 g_{3,3} p_{3,1} \\ & + 24a_{1,1} a_{2,2} b_3 p_{2,1} p_{3,1} + 12a_{1,1} a_{2,2} b_3 p_{2,2} p_{3,1} \\ & + 12a_{1,1} b_3 g_{1,1} p_{3,2} - 6a_{2,1} b_3 g_{2,1} p_{3,2} + 8a_{1,1} b_3 g_{3,3} p_{3,2} \\ & - 4a_{2,1} b_3 g_{3,3} p_{3,2} + 12a_{1,1} a_{2,2} b_3 p_{2,1} p_{3,2} \\ & + 6a_{1,1} a_{2,2} b_3 p_{2,2} p_{3,2} + 4a_{1,1} b_3 g_{1,1} p_{3,3} \\ & - 2a_{2,1} b_3 g_{2,1} p_{3,3} + 2a_{1,1} b_3 g_{3,3} p_{3,3} - a_{2,1} b_3 g_{3,3} p_{3,3} \\ & + 4a_{1,1} a_{2,2} b_3 p_{2,1} p_{3,3} + 2a_{1,1} a_{2,2} b_3 p_{2,2} p_{3,3}) = 0 \end{aligned}$
τ_9^W	4	$\begin{aligned} & \frac{1}{12} (12a_{1,1}^3 b_2 p_{2,1} p_{1,1}^3 + 6a_{1,1}^3 b_2 p_{2,2} p_{1,1}^3 - 24a_{1,1}^3 b_3 p_{3,1} p_{1,1}^3 \\ & + 12a_{2,1}^3 b_3 p_{3,1} p_{1,1}^3 - 12a_{1,1}^3 b_3 p_{3,2} p_{1,1}^3 + 6a_{2,1}^3 b_3 p_{3,2} p_{1,1}^3 \\ & - 4a_{1,1}^3 b_3 p_{3,3} p_{1,1}^3 + 2a_{2,1}^3 b_3 p_{3,3} p_{1,1}^3 - 3) = 0 \end{aligned}$
τ_{10}^W	4	$\begin{aligned} & \frac{1}{24} (24a_{1,1} a_{2,1} a_{2,2} b_3 p_{2,1} p_{3,1} p_{1,1}^2 \\ & + 12a_{1,1} a_{2,1} a_{2,2} b_3 p_{2,2} p_{3,1} p_{1,1}^2 + 12a_{1,1} a_{2,1} a_{2,2} b_3 p_{2,1} p_{3,2} p_{1,1}^2 \\ & + 6a_{1,1} a_{2,1} a_{2,2} b_3 p_{2,2} p_{3,2} p_{1,1}^2 + 4a_{1,1} a_{2,1} a_{2,2} b_3 p_{2,1} p_{3,3} p_{1,1}^2 \\ & + 2a_{1,1} a_{2,1} a_{2,2} b_3 p_{2,2} p_{3,3} p_{1,1}^2 - 3) = 0 \end{aligned}$
τ_{11}^W	4	$\begin{aligned} & \frac{1}{12} p_{1,1}^2 (6b_2 g_{1,1} p_{2,1} a_{1,1}^2 + 3b_2 g_{1,1} p_{2,2} a_{1,1}^2 \\ & - 12b_3 g_{1,1} p_{3,1} a_{1,1}^2 - 6b_3 g_{1,1} p_{3,2} a_{1,1}^2 - 2b_3 g_{1,1} p_{3,3} a_{1,1}^2 \\ & - 12a_{2,1} a_{2,2} b_3 p_{2,1} p_{3,1} a_{1,1} - 6a_{2,1} a_{2,2} b_3 p_{2,2} p_{3,1} a_{1,1} \\ & - 6a_{2,1} a_{2,2} b_3 p_{2,1} p_{3,2} a_{1,1} - 3a_{2,1} a_{2,2} b_3 p_{2,2} p_{3,2} a_{1,1} \\ & - 2a_{2,1} a_{2,2} b_3 p_{2,1} p_{3,3} a_{1,1} - a_{2,1} a_{2,2} b_3 p_{2,2} p_{3,3} a_{1,1} \\ & + 6a_{2,1}^2 b_3 g_{2,1} p_{3,1} + 3a_{2,1}^2 b_3 g_{2,1} p_{3,2} + a_{2,1}^2 b_3 g_{2,1} p_{3,3}) = 0 \end{aligned}$
τ_{12}^W	4	$\begin{aligned} & \frac{1}{12} (12a_{1,1}^2 a_{2,2} b_3 p_{2,1} p_{3,1} p_{1,1}^2 + 6a_{1,1}^2 a_{2,2} b_3 p_{2,2} p_{3,1} p_{1,1}^2 \\ & + 6a_{1,1}^2 a_{2,2} b_3 p_{2,1} p_{3,2} p_{1,1}^2 + 3a_{1,1}^2 a_{2,2} b_3 p_{2,2} p_{3,2} p_{1,1}^2 \\ & + 2a_{1,1}^2 a_{2,2} b_3 p_{2,1} p_{3,3} p_{1,1}^2 + a_{1,1}^2 a_{2,2} b_3 p_{2,2} p_{3,3} p_{1,1}^2 - 1) = 0 \end{aligned}$

Tree	Order	Order Condition: $B^\#(y_{n+1}) - B^\#(y(t_n + h)) = 0$
$\tau_{1,3}^W$	4	$\begin{aligned} & \frac{1}{24} p_{1,1}^2 (12b_2 g_{3,2} p_{2,1} a_{1,1}^2 + 4b_2 g_{3,2} p_{2,2} a_{1,1}^2 \\ & - 24b_3 g_{3,3} p_{3,1} a_{1,1}^2 - 24a_{2,2} b_3 p_{2,1} p_{3,1} a_{1,1}^2 \\ & - 12a_{2,2} b_3 p_{2,2} p_{3,1} a_{1,1}^2 - 8b_3 g_{3,3} p_{3,2} a_{1,1}^2 \\ & - 12a_{2,2} b_3 p_{2,1} p_{3,2} a_{1,1}^2 - 6a_{2,2} b_3 p_{2,2} p_{3,2} a_{1,1}^2 \\ & - 2b_3 g_{3,3} p_{3,3} a_{1,1}^2 - 4a_{2,2} b_3 p_{2,1} p_{3,3} a_{1,1}^2 \\ & - 2a_{2,2} b_3 p_{2,2} p_{3,3} a_{1,1}^2 + 12a_{2,1}^2 b_3 g_{3,3} p_{3,1} \\ & + 4a_{2,1}^2 b_3 g_{3,3} p_{3,2} + a_{2,1}^2 b_3 g_{3,3} p_{3,3}) = 0 \end{aligned}$
τ_{14}^W	4	$-\frac{1}{24}$
τ_{15}^W	4	$\frac{1}{24} a_{1,1} a_{2,2} b_3 g_{1,1} p_{1,1} (2p_{2,1} + p_{2,2})(6p_{3,1} + 3p_{3,2} + p_{3,3}) = 0$
τ_{16}^W	4	$\frac{1}{36} a_{1,1} a_{2,2} b_3 g_{2,2} p_{1,1} (3p_{2,1} + p_{2,2})(6p_{3,1} + 3p_{3,2} + p_{3,3}) = 0$
τ_{17}^W	4	$\begin{aligned} & \frac{1}{72} p_{1,1} (12a_{1,1} b_2 p_{2,1} g_{1,1}^2 + 6a_{1,1} b_2 p_{2,2} g_{1,1}^2 \\ & - 24a_{1,1} b_3 p_{3,1} g_{1,1}^2 - 12a_{1,1} b_3 p_{3,2} g_{1,1}^2 - 4a_{1,1} b_3 p_{3,3} g_{1,1}^2 \\ & - 36a_{1,1} a_{2,2} b_3 p_{2,1} p_{3,1} g_{1,1} - 18a_{1,1} a_{2,2} b_3 p_{2,2} p_{3,1} g_{1,1} \\ & - 18a_{1,1} a_{2,2} b_3 p_{2,1} p_{3,2} g_{1,1} - 9a_{1,1} a_{2,2} b_3 p_{2,2} p_{3,2} g_{1,1} \\ & - 6a_{1,1} a_{2,2} b_3 p_{2,1} p_{3,3} g_{1,1} - 3a_{1,1} a_{2,2} b_3 p_{2,2} p_{3,3} g_{1,1} \\ & + 12a_{2,1} b_3 g_{2,1}^2 p_{3,1} - 36a_{1,1} a_{2,2} b_3 g_{2,2} p_{2,1} p_{3,1} \\ & - 12a_{1,1} a_{2,2} b_3 g_{2,2} p_{2,2} p_{3,1} + 6a_{2,1} b_3 g_{2,1}^2 p_{3,2} \\ & - 18a_{1,1} a_{2,2} b_3 g_{2,2} p_{2,1} p_{3,2} - 6a_{1,1} a_{2,2} b_3 g_{2,2} p_{2,2} p_{3,2} \\ & + 2a_{2,1} b_3 g_{2,1}^2 p_{3,3} - 6a_{1,1} a_{2,2} b_3 g_{2,2} p_{2,1} p_{3,3} \\ & - 2a_{1,1} a_{2,2} b_3 g_{2,2} p_{2,2} p_{3,3}) = 0 \end{aligned}$
τ_{18}^W	4	$\frac{1}{48} a_{1,1} a_{2,2} b_3 g_{3,3} p_{1,1} (2p_{2,1} + p_{2,2})(12p_{3,1} + 4p_{3,2} + p_{3,3}) = 0$

Tree	Order	Order Condition: $B^\#(y_{n+1}) - B^\#(y(t_n + h)) = 0$
τ_{19}^W	4	$\begin{aligned} & \frac{1}{48} p_{1,1} (12a_{1,1} b_2 g_{1,1} g_{3,2} p_{2,1} \\ & - 24a_{1,1} a_{2,2} b_3 g_{1,1} p_{3,1} p_{2,1} - 24a_{1,1} a_{2,2} b_3 g_{3,3} p_{3,1} p_{2,1} \\ & - 12a_{1,1} a_{2,2} b_3 g_{1,1} p_{3,2} p_{2,1} - 8a_{1,1} a_{2,2} b_3 g_{3,3} p_{3,2} p_{2,1} \\ & - 4a_{1,1} a_{2,2} b_3 g_{1,1} p_{3,3} p_{2,1} - 2a_{1,1} a_{2,2} b_3 g_{3,3} p_{3,3} p_{2,1} \\ & + 4a_{1,1} b_2 g_{1,1} g_{3,2} p_{2,2} - 24a_{1,1} b_3 g_{1,1} g_{3,3} p_{3,1} \\ & + 12a_{2,1} b_3 g_{2,1} g_{3,3} p_{3,1} - 12a_{1,1} a_{2,2} b_3 g_{1,1} p_{2,2} p_{3,1} \\ & - 12a_{1,1} a_{2,2} b_3 g_{3,3} p_{2,2} p_{3,1} - 8a_{1,1} b_3 g_{1,1} g_{3,3} p_{3,2} \\ & + 4a_{2,1} b_3 g_{2,1} g_{3,3} p_{3,2} - 6a_{1,1} a_{2,2} b_3 g_{1,1} p_{2,2} p_{3,2} \\ & - 4a_{1,1} a_{2,2} b_3 g_{3,3} p_{2,2} p_{3,2} - 2a_{1,1} b_3 g_{1,1} g_{3,3} p_{3,3} \\ & + a_{2,1} b_3 g_{2,1} g_{3,3} p_{3,3} - 2a_{1,1} a_{2,2} b_3 g_{1,1} p_{2,2} p_{3,3} \\ & - a_{1,1} a_{2,2} b_3 g_{3,3} p_{2,2} p_{3,3}) = 0 \end{aligned}$
τ_{20}^W	4	$\begin{aligned} & \frac{1}{720} p_{1,1} (120a_{1,1} b_2 p_{2,1} g_{3,2}^2 + 30a_{1,1} b_2 p_{2,2} g_{3,2}^2 \\ & - 240a_{1,1} b_3 g_{3,3}^2 p_{3,1} + 120a_{2,1} b_3 g_{3,3}^2 p_{3,1} \\ & - 360a_{1,1} a_{2,2} b_3 g_{2,2} p_{2,1} p_{3,1} \\ & - 360a_{1,1} a_{2,2} b_3 g_{3,3} p_{2,1} p_{3,1} \\ & - 120a_{1,1} a_{2,2} b_3 g_{2,2} p_{2,2} p_{3,1} \\ & - 180a_{1,1} a_{2,2} b_3 g_{3,3} p_{2,2} p_{3,1} - 60a_{1,1} b_3 g_{3,3}^2 p_{3,2} \\ & + 30a_{2,1} b_3 g_{3,3}^2 p_{3,2} - 180a_{1,1} a_{2,2} b_3 g_{2,2} p_{2,1} p_{3,2} \\ & - 120a_{1,1} a_{2,2} b_3 g_{3,3} p_{2,1} p_{3,2} - 60a_{1,1} a_{2,2} b_3 g_{2,2} p_{2,2} p_{3,2} \\ & - 60a_{1,1} a_{2,2} b_3 g_{3,3} p_{2,2} p_{3,2} - 12a_{1,1} b_3 g_{3,3}^2 p_{3,3} \\ & + 6a_{2,1} b_3 g_{3,3}^2 p_{3,3} - 60a_{1,1} a_{2,2} b_3 g_{2,2} p_{2,1} p_{3,3} \\ & - 30a_{1,1} a_{2,2} b_3 g_{3,3} p_{2,1} p_{3,3} - 20a_{1,1} a_{2,2} b_3 g_{2,2} p_{2,2} p_{3,3} \\ & - 15a_{1,1} a_{2,2} b_3 g_{3,3} p_{2,2} p_{3,3}) = 0 \end{aligned}$

Tree	Order	Order Condition: $B^\#(y_{n+1}) - B^\#(y(t_n + h)) = 0$
τ_{21}^W	4	$ \begin{aligned} & \frac{1}{720} p_{1,1} \left(30b_1 g_{3,1}^3 - 120a_{1,1} b_2 g_{1,1}^2 p_{2,1} \right. \\ & - 120a_{1,1} b_2 g_{3,2}^2 p_{2,1} \\ & - 180a_{1,1} b_2 g_{1,1} g_{3,2} p_{2,1} \\ & - 60a_{1,1} b_2 g_{1,1}^2 p_{2,2} - 30a_{1,1} b_2 g_{3,2}^2 p_{2,2} \\ & - 60a_{1,1} b_2 g_{1,1} g_{3,2} p_{2,2} \\ & + 240a_{1,1} b_3 g_{1,1}^2 p_{3,1} - 120a_{2,1} b_3 g_{2,1}^2 p_{3,1} \\ & + 240a_{1,1} b_3 g_{3,3}^2 p_{3,1} - 120a_{2,1} b_3 g_{3,3}^2 p_{3,1} \\ & + 360a_{1,1} b_3 g_{1,1} g_{3,3} p_{3,1} \\ & - 180a_{2,1} b_3 g_{2,1} g_{3,3} p_{3,1} \\ & + 360a_{1,1} a_{2,2} b_3 g_{1,1} p_{2,1} p_{3,1} \\ & + 360a_{1,1} a_{2,2} b_3 g_{2,2} p_{2,1} p_{3,1} \\ & + 360a_{1,1} a_{2,2} b_3 g_{3,3} p_{2,1} p_{3,1} \\ & + 180a_{1,1} a_{2,2} b_3 g_{1,1} p_{2,2} p_{3,1} \\ & + 120a_{1,1} a_{2,2} b_3 g_{2,2} p_{2,2} p_{3,1} \\ & + 180a_{1,1} a_{2,2} b_3 g_{3,3} p_{2,2} p_{3,1} \\ & + 120a_{1,1} b_3 g_{1,1}^2 p_{3,2} - 60a_{2,1} b_3 g_{2,1}^2 p_{3,2} \\ & + 60a_{1,1} b_3 g_{3,3}^2 p_{3,2} - 30a_{2,1} b_3 g_{3,3}^2 p_{3,2} \\ & + 120a_{1,1} b_3 g_{1,1} g_{3,3} p_{3,2} \\ & - 60a_{2,1} b_3 g_{2,1} g_{3,3} p_{3,2} \\ & + 180a_{1,1} a_{2,2} b_3 g_{1,1} p_{2,1} p_{3,2} \\ & + 180a_{1,1} a_{2,2} b_3 g_{2,2} p_{2,1} p_{3,2} \\ & + 120a_{1,1} a_{2,2} b_3 g_{3,3} p_{2,1} p_{3,2} \\ & + 90a_{1,1} a_{2,2} b_3 g_{1,1} p_{2,2} p_{3,2} \\ & + 60a_{1,1} a_{2,2} b_3 g_{2,2} p_{2,2} p_{3,2} \\ & + 60a_{1,1} a_{2,2} b_3 g_{3,3} p_{2,2} p_{3,2} \\ & + 40a_{1,1} b_3 g_{1,1}^2 p_{3,3} - 20a_{2,1} b_3 g_{2,1}^2 p_{3,3} \\ & + 12a_{1,1} b_3 g_{3,3}^2 p_{3,3} - 6a_{2,1} b_3 g_{3,3}^2 p_{3,3} \\ & + 30a_{1,1} b_3 g_{1,1} g_{3,3} p_{3,3} \\ & - 15a_{2,1} b_3 g_{2,1} g_{3,3} p_{3,3} \\ & + 60a_{1,1} a_{2,2} b_3 g_{1,1} p_{2,1} p_{3,3} \\ & + 60a_{1,1} a_{2,2} b_3 g_{2,2} p_{2,1} p_{3,3} \\ & + 30a_{1,1} a_{2,2} b_3 g_{3,3} p_{2,1} p_{3,3} \\ & + 30a_{1,1} a_{2,2} b_3 g_{1,1} p_{2,2} p_{3,3} \\ & + 20a_{1,1} a_{2,2} b_3 g_{2,2} p_{2,2} p_{3,3} \\ & \left. + 15a_{1,1} a_{2,2} b_3 g_{3,3} p_{2,2} p_{3,3} \right) = 0 \end{aligned} $

3.2. Construction of practical EPIRK-W integrators

We will focus on constructing EPIRK-W methods (11) with three stages. Such a method using an approximate Jacobian reads:

$$\begin{aligned} Y_1 &= y_n + a_{1,1} \psi_{1,1}(g_{1,1} h \mathbf{A}_n) h f(y_n), \\ Y_2 &= y_n + a_{2,1} \psi_{2,1}(g_{2,1} h \mathbf{A}_n) h f(y_n) + a_{2,2} \psi_{2,2}(g_{2,2} h \mathbf{A}_n) h \Delta^{(1)} r(y_n), \\ y_{n+1} &= y_n + b_1 \psi_{3,1}(g_{3,1} h \mathbf{A}_n) h f(y_n) + b_2 \psi_{3,2}(g_{3,2} h \mathbf{A}_n) h \Delta^{(1)} r(y_n) \\ &\quad + b_3 \psi_{3,3}(g_{3,3} h \mathbf{A}_n) h \Delta^{(2)} r(y_n). \end{aligned} \tag{12}$$

An important observation from Table 3 is that the difference between the B-series coefficients of the exact solution and of the numerical solution corresponding to τ_{14}^W is equal to $-1/24$ and cannot be zeroed out. Since τ_{14}^W has only meagre nodes it appears in the B-series expansions of both the exact solution and the numerical solution. The conclusion is that three stage EPIRK-W methods with the simplified choice of $\psi_{i,j}(z)$ given in equation (9) cannot achieve order four. Consequently, we will limit our solution procedure to constructing third order EPIRK-W methods by zeroing out the first eight order conditions corresponding to TW -trees of up to order three. We use **Mathematica**[®] to solve the order conditions using two different approaches, as discussed next.

First approach to solving the order conditions. In the first approach we seek to make the terms of each order condition as similar to another as possible. We start the solution process by noticing that the first order condition trivially reduces to the substitution $b_1 \rightarrow 1/p_{1,1}$. The substitution $p_{3,2} \rightarrow -2p_{3,1}$ will zero out the following four terms: $-12a_{1,1} b_3 p_{1,1} p_{3,1} + 6a_{2,1} b_3 p_{1,1} p_{3,1} - 6a_{1,1} b_3 p_{1,1} p_{3,2} + 3a_{2,1} b_3 p_{1,1} p_{3,2}$, in order conditions τ_2^W and τ_3^W and hence reducing the complexity of the two conditions. It is immediately observed that $g_{3,1} \rightarrow 1$ as all the other terms in order conditions τ_2^W and τ_3^W are the same. Additionally, we make a choice that $g_{3,3} \rightarrow 0$. After making the substitutions, we solve order condition τ_2^W or τ_3^W to get,

$$p_{3,3} \rightarrow \frac{3(2a_{1,1} b_2 p_{1,1} p_{2,1} + a_{1,1} b_2 p_{1,1} p_{2,2} - 1)}{b_3 p_{1,1} (2a_{1,1} - a_{2,1})}.$$

This substitution results in a number of terms in multiple order conditions having the expression $(2a_{1,1} - a_{2,1})$ in the denominator. So we arbitrarily choose $a_{2,1} \rightarrow 2a_{1,1} - 1$. The order conditions are far simpler now with several terms having the factor $(-1 + 2a_{1,1})$ and its powers in their expression. We choose $a_{1,1} \rightarrow 1/2$. Following this substitution, we can solve from order condition τ_4^W that $p_{1,1} \rightarrow 4/3$. After plugging in the value for $p_{1,1}$, order conditions τ_5^W and τ_6^W suggest that $g_{1,1} \rightarrow 2/3$. Now order conditions τ_5^W , τ_6^W , τ_7^W and τ_8^W have the following coefficients as part of their expressions: $a_{2,2}$, $p_{2,1}$, $p_{2,2}$, $g_{3,2}$ and b_2 . We arbitrarily set $p_{2,2} \rightarrow 2p_{2,1}$ and solve for the remaining coefficients to obtain

$$b_2 \rightarrow \frac{3a_{2,2} p_{2,1} + 1}{8a_{2,2} p_{2,1}^2} \quad \text{and} \quad g_{3,2} \rightarrow \frac{12a_{2,2} p_{2,1}}{5(3a_{2,2} p_{2,1} + 1)}.$$

We now select arbitrary values for some of the remaining coefficients. We choose $p_{2,1} \rightarrow 1$, $a_{2,2} \rightarrow 1$, $b_3 \rightarrow 1$, $a_{1,2} \rightarrow 0$, $a_{1,3} \rightarrow 0$, $a_{2,3} \rightarrow 0$, $p_{3,1} \rightarrow 0$, $p_{2,3} \rightarrow 0$, $p_{1,2} \rightarrow 0$, $p_{1,3} \rightarrow 0$, $g_{1,2} \rightarrow 0$, $g_{1,3} \rightarrow 0$, $g_{2,1} \rightarrow 0$, $g_{2,2} \rightarrow 0$, and $g_{2,3} \rightarrow 0$.

In order to solve for a second order embedded method we rewrite the final stage of the method with new coefficients \hat{b}_i . Plugging in the substitutions that have been arrived at while solving the order conditions for the third order method results in a set of new conditions in only the \hat{b}_i . It is again straightforward to observe that $\hat{b}_1 \rightarrow 1/p_{1,1}$. We next solve the conditions for TW -trees up to order = 2. Solving order conditions τ_2^W and τ_3^W we get $\hat{b}_3 \rightarrow -3 + 8\hat{b}_2$.

The resulting coefficients for a third-order EPIRK-W method (EPIRKW3A) with an embedded second-order method are given in Figure 1. The choices that we have made for the coefficients a 's, b 's, g 's and p 's result in the sum of coefficients on trees τ_5^W , τ_6^W , τ_7^W and τ_8^W to sum to zero in the embedded method no matter what value is chosen for \hat{b}_2 . And when we choose $\mathbf{A}_n = \mathbf{J}_n$, the exact Jacobian, trees τ_5^W , τ_6^W , τ_7^W

Figure 1: Coefficients for EPIRKW3A

$$a = \begin{bmatrix} \frac{1}{2} & 0 & 0 \\ 0 & 1 & 0 \end{bmatrix}, \quad \begin{bmatrix} b \\ \hat{b} \end{bmatrix} = \begin{bmatrix} \frac{3}{4} & \frac{1}{2} & 1 \\ \frac{3}{4} & \frac{3}{4} & \frac{6}{5} \end{bmatrix}, \quad g = \begin{bmatrix} \frac{2}{3} & 0 & 0 \\ 0 & 0 & 0 \\ 1 & \frac{3}{5} & 0 \end{bmatrix}, \quad p = \begin{bmatrix} \frac{4}{3} & 0 & 0 \\ 1 & 2 & 0 \\ 0 & 0 & \frac{3}{4} \end{bmatrix}.$$

and τ_8^W are the same tree and it turns out that we incidentally solve the embedded method up to third order as well. To work around this restriction, we need to have the a 's, g 's and p 's to be independent of the b 's and to solve separately for the \hat{b} 's to ensure that we get a second-order embedded method.

Second approach to solving the order conditions. In this approach we impose a horizontal structure on the g coefficients akin to the horizontally adaptive method described in [15]. In order to impose a horizontal structure on g we make the following substitutions: $g_{1,2} \rightarrow g_{1,1}$, $g_{1,3} \rightarrow g_{1,1}$, $g_{2,2} \rightarrow g_{2,1}$, $g_{2,3} \rightarrow g_{2,1}$, $g_{3,2} \rightarrow g_{3,1}$, and $g_{3,3} \rightarrow g_{3,1}$. We also note that the first order condition reduces to $b_1 \rightarrow 1/p_{1,1}$ again. Order-conditions τ_2^W and τ_3^W imply $g_{3,1} \rightarrow 1$. We solve order-conditions τ_2^W and τ_3^W and get two possible solutions for a subset of the variables. We plugin the first solution and solve order conditions τ_4^W , τ_5^W and τ_6^W . We again get multiple solutions and we use the first solution to substitute into the order conditions and proceed to solve order conditions τ_7^W and τ_8^W . We again get multiple solutions for the remaining coefficients. One of the solutions returned by **Mathematica**[®] gives a non-singular system, and using it leads to the following family of order three method coefficients:

$$\begin{aligned} g_{1,2} &\rightarrow g_{1,1}, g_{1,3} \rightarrow g_{1,1}, g_{2,2} \rightarrow g_{2,1}, g_{2,3} \rightarrow g_{2,1}, g_{3,2} \rightarrow g_{3,1}, g_{3,3} \rightarrow g_{3,1}, \\ b_1 &\rightarrow \frac{1}{p_{1,1}}, b_2 \rightarrow -\frac{a_{2,2}(3a_{2,1}p_{1,1} - 4)}{2a_{2,1}^2 p_{1,1}^2}, b_3 \rightarrow -\frac{3a_{2,1}p_{1,1} - 4}{a_{2,1}^2 p_{1,1}^2 (6p_{3,1} + 3p_{3,2} + p_{3,3})}, \\ p_{2,1} &\rightarrow 0, a_{1,1} \rightarrow \frac{a_{2,1}}{2}, g_{3,1} \rightarrow 1, g_{2,1} \rightarrow \frac{2(3a_{2,1}g_{1,1}p_{1,1} - a_{2,1}p_{1,1} - 2g_{1,1})}{3a_{2,1}p_{1,1} - 4}, \\ p_{2,2} &\rightarrow -\frac{2(9a_{1,1}a_{2,1}a_{2,2}p_{1,1}p_{2,1} - 6a_{1,1}a_{2,1}p_{1,1} - 12a_{1,1}a_{2,2}p_{2,1} + 8a_{1,1} + 6a_{2,1}^2 p_{1,1} - 4a_{2,1})}{3a_{1,1}a_{2,2}(3a_{2,1}p_{1,1} - 4)}. \end{aligned} \quad (13)$$

After making the above substitutions in the embedded method, we obtain the following solutions for the embedded coefficients:

$$\hat{b}_1 \rightarrow \frac{1}{p_{1,1}}, \quad \hat{b}_2 \rightarrow -\frac{a_{2,2}(3a_{2,1}p_{1,1} - 4)}{2a_{2,1}^2 p_{1,1}^2},$$

with \hat{b}_3 a free parameter that can be chosen to obtain a second order embedded method.

A solution to the above family leads to the third order EPIRK- W method (EPIRKW3B) in Figure 2, with a second order embedded method that overcomes the limitation of the embedded method of EPIRKW3A.

4. EPIRK- K methods

W -methods have the advantage that any approximation of the Jacobian that ensures stability can be used, therefore they have the potential for attaining excellent computational efficiency in comparison to methods that require exact Jacobians. The drawback of the W -methods, however, is the very large number of order conditions that need to be solved for constructing the method [7, Section IV.7].

In order to reduce the number of order conditions Krylov-based methods (K -methods) were developed for Rosenbrock integrators in [26] and for exponential integrators in [25]. K -methods are built in the framework of W -methods and use a very specific approximation to the Jacobian constructed in the Krylov space. This approximation allows TW -trees with linear sub-trees having fat root to be re-colored (as meagre), leading

Figure 2: Coefficients for EPIRKW3B

$$\begin{aligned}
a &= \begin{bmatrix} 0.22824182961171620396 & 0 & 0 \\ 0.45648365922343240794 & 0.33161664063356950085 & 0 \end{bmatrix}, \\
b &= \begin{bmatrix} 1 \\ 2.0931591383832578214 \\ 1.2623969257900804404 \end{bmatrix}^T, \\
\hat{b} &= \begin{bmatrix} 1 \\ 2.0931591383832578214 \\ 1 \end{bmatrix}^T, \\
g &= \begin{bmatrix} 0 & 0 & 0 \\ 0.34706341174296320958 & 0.34706341174296320958 & 0.34706341174296320958 \\ 1 & 1 & 1 \end{bmatrix}, \\
p &= \begin{bmatrix} 1 & 0 & 0 \\ 0 & 2.0931604100438501004 & 0 \\ 1 & 1 & 1 \end{bmatrix}.
\end{aligned}$$

to the new class of *TK*-trees. The recoloring results in substantially fewer trees, and therefore fewer order conditions for the *K*-methods [26, Lemma 3.2, 3.3].

In this section we derive *K*-methods in the framework of EPIRK integrators.

4.1. Krylov-subspace approximation of Jacobian

K-methods build the Krylov-subspace *M*-dimensional Krylov-subspace \mathcal{K}_M , $M \ll N$, based on the exact Jacobian \mathbf{J}_n and the ODE function value f_n at the current time step t_n :

$$\mathcal{K}_M = \text{span}\{f_n, \mathbf{J}_n f_n, \mathbf{J}_n^2 f_n, \dots, \mathbf{J}_n^{M-1} f_n\}. \quad (14)$$

The modified Arnoldi iteration [27] computes an orthonormal basis \mathbf{V} and upper-Hessenberg matrix \mathbf{H} such that:

$$\mathcal{K}_M = \text{span}\{v_1, \dots, v_M\}, \quad \mathbf{V} = [v_1, \dots, v_M] \in \mathbb{R}^{N \times M}, \quad \mathbf{V}^T \mathbf{V} = \mathbf{I}_M, \quad \mathbf{H} = \mathbf{V}^T \mathbf{J}_n \mathbf{V} \in \mathbb{R}^{M \times M}. \quad (15)$$

Using \mathbf{H} and \mathbf{V} the approximation of the Jacobian matrix \mathbf{J}_n in the Krylov sub-space is defined as

$$\mathbf{A}_n = \mathbf{V} \mathbf{H} \mathbf{V}^T = \mathbf{V} \mathbf{V}^T \mathbf{J}_n \mathbf{V} \mathbf{V}^T \in \mathbb{R}^{N \times N}. \quad (16)$$

This approximation of the Jacobian is used by *K*-methods. The important properties of this approximation are given by the following Lemmas from [25].

Lemma 4.1 (Powers of \mathbf{A}_n [25]). *Powers of \mathbf{A}_n : $\mathbf{A}_n^k = \mathbf{V} \mathbf{H}^k \mathbf{V}^T$ for any $k \geq 1$.*

Lemma 4.2 (Evaluation of φ functions (5) on the approximate Jacobian (16) [25]). *We have that:*

$$\varphi_k(h \gamma \mathbf{A}_n) = \frac{1}{k!} (\mathbf{I}_N - \mathbf{V} \mathbf{V}^T) + \mathbf{V} \varphi_k(h \gamma \mathbf{H}) \mathbf{V}^T, \quad k = 1, 2, \dots$$

In order to derive the Krylov formulation of the EPIRK methods (12) we need to extend Lemma 4.2 to the evaluation of ψ functions (9). We have the following result.

Lemma 4.3 (Evaluation of ψ functions (9) on the approximate Jacobian (16)).

$$\psi_j(h \gamma \mathbf{A}_n) = \tilde{p}_j (\mathbf{I}_N - \mathbf{V} \mathbf{V}^T) + \mathbf{V} \psi_j(h \gamma \mathbf{H}) \mathbf{V}^T, \quad j = 1, 2, \dots \quad \text{where} \quad \tilde{p}_j = \sum_{k=1}^j \frac{p_{j,k}}{k!}.$$

Proof. From the definition (9) we have:

$$\begin{aligned}
\psi_j(h\gamma\mathbf{A}_n) &= \sum_{k=1}^j p_{j,k} \varphi_k(h\gamma\mathbf{A}_n) \\
&= \sum_{k=1}^j p_{j,k} \left[\frac{1}{k!} (\mathbf{I}_N - \mathbf{V}\mathbf{V}^T) + \mathbf{V} \varphi_k(h\gamma\mathbf{H}) \mathbf{V}^T \right] \\
&= (\mathbf{I}_N - \mathbf{V}\mathbf{V}^T) \left[\sum_{k=1}^j \frac{p_{j,k}}{k!} \right] + \mathbf{V} \psi_j(h\gamma\mathbf{H}) \mathbf{V}^T \\
&= \tilde{p}_j(\mathbf{I}_N - \mathbf{V}\mathbf{V}^T) + \mathbf{V} \psi_j(h\gamma\mathbf{H}) \mathbf{V}^T.
\end{aligned}$$

□

4.2. Formulation of EPIRK-K methods

We now derive the Krylov-subspace formulation of the EPIRK methods, which will be called EPIRK-K methods. For this we begin with the EPIRK-W formulation (11) and use the Jacobian approximation (16). The first step in the method derivation is to split all vectors appearing in the method formulation (11) into components within the Krylov-subspace and components orthogonal to it, as follows:

1. Splitting the internal stage vectors leads to:

$$Y_i = \mathbf{V}\lambda_i + Y_i^\perp \quad \text{where} \quad \mathbf{V}^T Y_i = \lambda_i, \quad (\mathbf{I}_N - \mathbf{V}\mathbf{V}^T) Y_i = Y_i^\perp, \quad (17)$$

where $Y_0 \equiv y_n$.

2. Splitting the right-hand side function evaluated at the internal stage vectors gives:

$$f_i := f(Y_i) = \mathbf{V}\eta_i + f_i^\perp \quad \text{where} \quad \mathbf{V}^T f_i = \eta_i, \quad (\mathbf{I}_N - \mathbf{V}\mathbf{V}^T) f_i = f_i^\perp, \quad (18)$$

where $f_0 \equiv f(y_n)$.

3. Splitting the non-linear Taylor remainder terms of the right-hand side functions yields:

$$\begin{aligned}
r(Y_i) &= f(Y_i) - f(y_n) - \mathbf{A}_n(Y_i - y_n) = f_i - f_0 - \mathbf{V}\mathbf{H}\mathbf{V}^T(Y_i - y_n), \\
\text{where } \mathbf{V}^T r(Y_i) &= \eta_i - \eta_0 - \mathbf{H}(\lambda_i - \lambda_0), \\
(\mathbf{I}_N - \mathbf{V}\mathbf{V}^T) r(Y_i) &= f_i^\perp - f_0^\perp.
\end{aligned} \quad (19)$$

4. Splitting the forward differences of the non-linear remainder terms leads to:

$$\begin{aligned}
\tilde{r}_{(j-1)} &:= \Delta^{(j-1)} r(y_n) = \mathbf{V} d_{(j-1)} + \tilde{r}_{(j-1)}^\perp, \\
\text{where } \mathbf{V}^T \tilde{r}_{(j-1)} &= d_{(j-1)}, \quad (\mathbf{I}_N - \mathbf{V}\mathbf{V}^T) \tilde{r}_{(j-1)} = \tilde{r}_{(j-1)}^\perp.
\end{aligned} \quad (20)$$

In the above equations, $\mathbf{V}\lambda_i$, $\mathbf{V}\eta_i$ and $\mathbf{V}d_{(j-1)}$ are components of Y_i , f_i and $\Delta^{(j-1)}r(y_n)$ in the Krylov-subspace, whereas Y_i^\perp , f_i^\perp and $\tilde{r}_{(j-1)}^\perp$ lie in the orthogonal subspace.

Using the above equations and Lemma 4.3, the intermediate stage equations of the method (11)

$$Y_i = y_n + a_{i,1} \psi_1(g_{i,1} h \mathbf{V}\mathbf{H}\mathbf{V}^T) h f(y_n) + \sum_{j=2}^i a_{i,j} \psi_j(g_{i,j} h \mathbf{V}\mathbf{H}\mathbf{V}^T) h \Delta^{(j-1)} r(y_n), \quad (21)$$

become:

$$\begin{aligned} Y_i = \mathbf{V}\lambda_i + Y_i^\perp &= y_n + h a_{i,1} \left(\tilde{p}_1 (f_0 - \mathbf{V}\eta_0) + \mathbf{V}\psi_1(h g_{i,1} \mathbf{H})\eta_0 \right) \\ &\quad + \sum_{j=2}^i h a_{i,j} \left(\tilde{p}_j \tilde{r}_{(j-1)}^\perp + \mathbf{V}\psi_j(h g_{i,j} \mathbf{H}) d_{(j-1)} \right), \end{aligned} \quad (22)$$

where $\tilde{r}_{(j-1)}^\perp$ and $d_{(j-1)}$ can be proved to be, as is done in appendix B,

$$d_{(j-1)} = \sum_{k=0}^{j-1} \left((-1)^k \binom{j-1}{k} \eta_{j-1-k} - \mathbf{H} \left((-1)^k \binom{j-1}{k} \lambda_{j-1-k} \right) \right), \quad (23a)$$

$$\tilde{r}_{(j-1)}^\perp = \sum_{k=0}^{j-1} \left((-1)^k \binom{j-1}{k} (f_{j-1-k} - \mathbf{V}\eta_{j-1-k}) \right). \quad (23b)$$

The reduced stage vector for the K -method is obtained by multiplying the full stage vector in equation (22) by \mathbf{V}^T from the left,

$$\lambda_i = \lambda_0 + h a_{i,1} \psi_1(h g_{i,1} \mathbf{H}) \eta_0 + \sum_{j=2}^i h a_{i,j} \psi_j(h g_{i,j} \mathbf{H}) d_{(j-1)}, \quad (24)$$

and the component of the full stage vector, when multiplied by $(I - \mathbf{V}\mathbf{V}^T)$, in the orthogonal subspace is,

$$Y_i^\perp = (y_n - \mathbf{V}\lambda_0) + h a_{i,1} \tilde{p}_1 (f_0 - \mathbf{V}\eta_0) + \sum_{j=2}^i h a_{i,j} \tilde{p}_j \tilde{r}_{(j-1)}^\perp. \quad (25)$$

The full-stage vector can be recovered by first projecting the reduced stage vector λ_i back into full space and adding the piece that is orthogonal to it, Y_i^\perp , as done in equation (22).

Similarly, the computation of the next solution in the method (11)

$$y_{n+1} = y_n + b_1 \psi_{s,1}(g_{s,1} h \mathbf{A}_n) h f(y_n) + \sum_{j=2}^s b_j \psi_{s,j}(g_{s,j} h \mathbf{A}_n) h \Delta^{(j-1)} r(y_n), \quad (26)$$

becomes:

$$y_{n+1} = V\lambda_s + y_{n+1}^\perp, \quad (27)$$

where

$$\lambda_s = \lambda_0 + h b_1 \psi_1(h g_{s,1} \mathbf{H}) \eta_0 + \sum_{j=2}^s h b_j \psi_j(h g_{s,j} \mathbf{H}) d_{(j-1)}, \quad (28)$$

and

$$y_{n+1}^\perp = (y_n - \mathbf{V}\lambda_0) + h b_1 \tilde{p}_1 (f_0 - \mathbf{V}\eta_0) + \sum_{j=2}^s h b_j \tilde{p}_j \tilde{r}_{(j-1)}^\perp. \quad (29)$$

One step of the resulting EPIRK- K method (for an autonomous system) is summarized in Algorithm 2.

4.3. Order conditions theory for EPIRK- K methods

K -methods construct a single Krylov-subspace per timestep, and use it to approximate the Jacobian. All stage vectors are also computed in this reduced space, before being projected back into the full space between successive stages. The order condition theory accounts for this computational procedure [26, Theorem 3.6].

Before we discuss the order conditions for the K -methods, we define the trees that arise in the expansion of their solutions. Recalling that a linear tree is one where each node has only one child, consider the following definition:

Algorithm 2 EPIRK- K

```

1:  $f_0 := f(y_n)$  ▷ Repeat for every timestep in the timespan
2:  $\mathbf{J}_n := \mathbf{J}(y_n)$ 
3:  $[\mathbf{H}, \mathbf{V}] = \text{Arnoldi}(\mathbf{J}_n, f_0)$ 
4:  $\lambda_0 = \mathbf{V}^T y_n$ 
5:  $\eta_0 = \mathbf{V}^T f_0$ 
6: for  $i = 1 : s - 1$  do ▷ Do for each stage of the method
7:    $d_{(i-1)} = \begin{cases} 0 & , \text{ if } i = 1 \\ \sum_{k=0}^{i-1} \left( (-1)^k \binom{i-1}{k} \eta_{i-1-k} - \mathbf{H} \left( (-1)^k \binom{i-1}{k} \lambda_{i-1-k} \right) \right) & , \text{ if } i \geq 2 \end{cases}$ 
8:    $\tilde{r}_{(i-1)}^\perp = \begin{cases} 0 & , \text{ if } i = 1 \\ \sum_{k=0}^{i-1} \left( (-1)^k \binom{i-1}{k} (f_{i-1-k} - \mathbf{V} \eta_{i-1-k}) \right) & , \text{ if } i \geq 2 \end{cases}$ 
9:    $\lambda_i = \lambda_0 + h a_{i,1} \psi_1(h g_{i,1} \mathbf{H}) \eta_0 + \sum_{j=2}^i h a_{i,j} \psi_j(h g_{i,j} \mathbf{H}) d_{(j-1)}$ 
10:   $Y_i = \mathbf{V} \lambda_i + (y_n - \mathbf{V} \lambda_0) + h a_{i,1} \tilde{p}_1 (f_0 - \mathbf{V} \eta_0) + \sum_{j=2}^i h a_{i,j} \tilde{p}_j \tilde{r}_{(j-1)}^\perp$ 
11:   $f_i = f(Y_i)$ 
12:   $\eta_i = \mathbf{V}^T f_i$ 
13: end for
14:  $d_{(s-1)} = \sum_{k=0}^{s-1} \left( (-1)^k \binom{s-1}{k} \eta_{s-1-k} - \mathbf{H} \left( (-1)^k \binom{s-1}{k} \lambda_{s-1-k} \right) \right)$ 
15:  $\tilde{r}_{(s-1)}^\perp = \sum_{k=0}^{s-1} \left( (-1)^k \binom{s-1}{k} (f_{s-1-k} - \mathbf{V} \eta_{s-1-k}) \right)$ 
16:  $\lambda_s = \lambda_0 + h b_1 \psi_1(h g_{s,1} \mathbf{H}) \eta_0 + \sum_{j=2}^s h b_j \psi_j(h g_{s,j} \mathbf{H}) d_{(j-1)}$ 
17:  $y_{n+1} = \mathbf{V} \lambda_s + (y_n - \mathbf{V} \lambda_0) + h b_1 \tilde{p}_1 (f_0 - \mathbf{V} \eta_0) + \sum_{j=2}^s h b_j \tilde{p}_j \tilde{r}_{(j-1)}^\perp$ 

```

Definition 4.4 (TK-Trees [26]).

$$TK = \left\{ TW\text{-trees: no linear sub-tree has a fat (empty) root} \right\}.$$

$$TK(k) = \left\{ TW\text{-trees: no linear sub-tree of order less than or equal to } k \text{ has a fat (empty) root} \right\}.$$

Theorem 4.5. *Trees corresponding to series expansion of the numerical solution of K -method with Krylov-subspace dimension M are $TK(M)$.*

Proof. Using lemmas 4.1, 4.2, 4.3, and [25, Lemmas 3, 4] we arrive at the desired result. \square

The order conditions are derived from matching the coefficients of the B-series expansion of the numerical solution to those of the B-series expansion of the exact solution. If the expansion is made in the elementary differentials corresponding to the TK trees, then for a fourth order method there is a single additional tree (τ_8^K) in the numerical solution having both meagre and fat nodes in comparison to the T -trees up to order four for a classical EPIRK method. In contrast with the W -method that had twenty-one order conditions, the K -method has just nine for a fourth order method, which is almost the same as a classical EPIRK having eight.

As mentioned earlier, TK -trees come from re-coloring all the linear sub-trees with a fat root as meagre in the TW -trees. This significantly reduces the number of order conditions for the K -method since groups of TW -trees become isomorphic to one another after recoloring. TK -trees up to order four are given in [25]. This also indicates that the coefficients in front of these TK -trees in the B-series expansion can be obtained by summing together the coefficients of TW -trees, which become isomorphic to one another, from the corresponding expansion.

The order four conditions for EPIRK- K methods with three stages (12) are discussed next and are summarized in Table 4.

Table 4: Order conditions for the three stage EPIRK- K method

Tree #	Order	Order Condition: $B^\#(y_{n+1}) - B^\#(y(t_n + h)) = 0$
τ_1^K	1	$b_1 p_{1,1} - 1 = 0$
τ_2^K	2	$\frac{1}{2}(b_1 g_{3,1} p_{1,1} - 1) = 0$
τ_3^K	3	$\frac{1}{6}(6a_{1,1}^2 b_2 p_{1,1}^2 p_{2,1} + 3a_{1,1}^2 b_2 p_{1,1}^2 p_{2,2} - 12a_{1,1}^2 b_3 p_{1,1}^2 p_{3,1} - 6a_{1,1}^2 b_3 p_{1,1}^2 p_{3,2} - 2a_{1,1}^2 b_3 p_{1,1}^2 p_{3,3} + 6a_{2,1}^2 b_3 p_{1,1}^2 p_{3,1} + 3a_{2,1}^2 b_3 p_{1,1}^2 p_{3,2} + a_{2,1}^2 b_3 p_{1,1}^2 p_{3,3} - 2) = 0$
τ_4^K	3	$\frac{1}{6}(b_1 g_{3,1}^2 p_{1,1} - 1) = 0$

Tree #	Order	Order Condition: $B^\#(y_{n+1}) - B^\#(y(t_n + h)) = 0$
τ_5^K	4	$\frac{1}{12} (12a_{1,1}^3 b_2 p_{1,1}^3 p_{2,1} + 6a_{1,1}^3 b_2 p_{1,1}^3 p_{2,2} - 24a_{1,1}^3 b_3 p_{1,1}^3 p_{3,1} - 12a_{1,1}^3 b_3 p_{1,1}^3 p_{3,2} - 4a_{1,1}^3 b_3 p_{1,1}^3 p_{3,3} + 12a_{2,1}^3 b_3 p_{1,1}^3 p_{3,1} + 6a_{2,1}^3 b_3 p_{1,1}^3 p_{3,2} + 2a_{2,1}^3 b_3 p_{1,1}^3 p_{3,3} - 3) = 0$
τ_6^K	4	$\frac{1}{24} (12a_{1,1}^2 b_2 g_{1,1} p_{1,1}^2 p_{2,1} + 6a_{1,1}^2 b_2 g_{1,1} p_{1,1}^2 p_{2,2} - 24a_{1,1}^2 b_3 g_{1,1} p_{1,1}^2 p_{3,1} - 12a_{1,1}^2 b_3 g_{1,1} p_{1,1}^2 p_{3,2} - 4a_{1,1}^2 b_3 g_{1,1} p_{1,1}^2 p_{3,3} + 12a_{2,1}^2 b_3 g_{2,1} p_{1,1}^2 p_{3,1} + 6a_{2,1}^2 b_3 g_{2,1} p_{1,1}^2 p_{3,2} + 2a_{2,1}^2 b_3 g_{2,1} p_{1,1}^2 p_{3,3} - 3) = 0$
τ_7^K	4	$\frac{1}{12} (12a_{1,1}^2 a_{2,2} b_3 p_{1,1}^2 p_{2,1} p_{3,1} + 6a_{1,1}^2 a_{2,2} b_3 p_{1,1}^2 p_{2,1} p_{3,2} + 2a_{1,1}^2 a_{2,2} b_3 p_{1,1}^2 p_{2,1} p_{3,3} + 6a_{1,1}^2 a_{2,2} b_3 p_{1,1}^2 p_{2,2} p_{3,1} + 3a_{1,1}^2 a_{2,2} b_3 p_{1,1}^2 p_{2,2} p_{3,2} + a_{1,1}^2 a_{2,2} b_3 p_{1,1}^2 p_{2,2} p_{3,3} - 1) = 0$
τ_8^K	4	$\frac{1}{24} p_{1,1}^2 (-24a_{1,1}^2 a_{2,2} b_3 p_{2,1} p_{3,1} - 12a_{1,1}^2 a_{2,2} b_3 p_{2,1} p_{3,2} - 4a_{1,1}^2 a_{2,2} b_3 p_{2,1} p_{3,3} - 12a_{1,1}^2 a_{2,2} b_3 p_{2,2} p_{3,1} - 6a_{1,1}^2 a_{2,2} b_3 p_{2,2} p_{3,2} - 2a_{1,1}^2 a_{2,2} b_3 p_{2,2} p_{3,3} + 12a_{1,1}^2 b_2 g_{3,2} p_{2,1} + 4a_{1,1}^2 b_2 g_{3,2} p_{2,2} - 24a_{1,1}^2 b_3 g_{3,3} p_{3,1} - 8a_{1,1}^2 b_3 g_{3,3} p_{3,2} - 2a_{1,1}^2 b_3 g_{3,3} p_{3,3} + 12a_{2,1}^2 b_3 g_{3,3} p_{3,1} + 4a_{2,1}^2 b_3 g_{3,3} p_{3,2} + a_{2,1}^2 b_3 g_{3,3} p_{3,3}) = 0$
τ_9^K	4	$\frac{1}{24} (b_1 g_{3,1}^3 p_{1,1} - 1) = 0$

Corollary 4.6. Any EPIRK-K-method of order p gives rise to a classical EPIRK method of order p (with the same coefficients).

Proof. The proof follows directly from comparing the set of T -trees to TK -trees. \square

Corollary 4.7. Any classical EPIRK method of order $p \geq 3$ gives rise to an equivalent K -method of order at least three (with the same coefficients).

Proof. The proof follows directly from comparing the set of T -trees to TK -trees. \square

4.4. Construction of practical EPIRK-K integrators

Note that order condition τ_8^K is the additional order condition that was mentioned earlier whose TW -tree could not be re-colored according to [26, Lemma 3.2, 3.3]. This is the only tree that is not present in

T -trees up to order 4, and therefore we impose that the associated coefficient is equal to zero. To solve the order conditions we use **Mathematica**[®] and the solution procedure described for the first variant of EPIRK- W method where we make terms of each order condition similar to one another by making suitable substitutions. We arrive at the EPIRK- K method (EPIRKK4) of order four in Figure 3, with an embedded method of order three.

Figure 3: Coefficients for EPIRKK4

$$a = \begin{bmatrix} \frac{692665874901013}{799821658665135} & 0 & 0 \\ \frac{692665874901013}{799821658665135} & \frac{3}{4} & 0 \end{bmatrix}, \quad \begin{bmatrix} b \\ \widehat{b} \end{bmatrix} = \begin{bmatrix} \frac{799821658665135}{692665874901013} & \frac{352}{729} & \frac{64}{729} \\ \frac{799821658665135}{692665874901013} & \frac{32}{81} & 0 \end{bmatrix},$$

$$g = \begin{bmatrix} \frac{3}{4} & 0 & 0 \\ \frac{3}{4} & 0 & 0 \\ 1 & \frac{9}{16} & \frac{9}{16} \end{bmatrix}, \quad p = \begin{bmatrix} \frac{692665874901013}{799821658665135} & 0 & 0 \\ 1 & 1 & 0 \\ 1 & 1 & 0 \end{bmatrix}.$$

The theory of K -methods gives a lower bound on the Krylov-subspace size that guarantees the order of convergence [26, Theorem 3.6]. This bound depends only on the order of convergence of the method and not on the dimension of the ODE system.

Here we have constructed a fourth order EPIRK- K method in Figure 3, which requires a Krylov-subspace of dimension four [26, Theorem 3.6]. All expensive operations such as computing products of ψ function of matrices with vectors are performed in this reduced space. Significant computational advantages are obtained if the Krylov-subspace captures all the stiff eigenmodes of the system. If not all stiff eigenmodes are captured, stability requirements will force the integrator to take smaller timesteps, which will increase the overall cost of integration. In such cases we typically observe that adding more vectors to the Krylov-subspace can improve the performance of the K -type integrator.

5. Implementation strategies for exponential integrators

An important part of the implementation of exponential integrators is the computation of products of φ or ψ functions of matrices with vectors. The choice of approximation used depends on the properties of the matrix and the type of exponential method under consideration. In this section, we briefly review the strategies used to evaluate these products in the context of the methods discussed in this paper. Table 5 lists these methods and the implementation framework used in each case. It includes the W -methods presented in Section 3, a fourth order K -method presented in Section 4, and several classical methods that have been implemented to perform comparative studies. In the following discussion we will use the terms implementation and integrator interchangeably, and the term method should be understood as the formulation along with the set of coefficients.

We first discuss the computation of these products for classical exponential integrators listed in Table 5. For EPIRKK4-CLASSICAL and EPIRK5 [21, Table 4, Equation 28] the evaluation of products of ψ functions with vectors proceeds by first approximating the individual φ function products in the Krylov-subspace as illustrated in [20, sec 3.1], i.e. $\varphi_k(h\gamma\mathbf{A}_n)b \approx \|b\|\mathbf{V}\varphi_k(h\gamma\mathbf{H})e_1$. The φ function products associated with the approximation, $\varphi_k(h\gamma\mathbf{H})e_1$, are computed by constructing an augmented matrix and exponentiating it as described in [18, Theorem 1]. Finally taking a linear combination of columns of the resulting matrix gives the ψ function product. In the augmented matrix approach, an Arnoldi iteration is needed for each new vector in the formulation given in equation (10). Each of the classical integrators listed above has three stages that work with three different vectors b , requiring three Arnoldi iterations per timestep. EPIRK5P1BVAR [23] and EROW4 [11, 22], which we include in our numerical experiments, also perform three Arnoldi projections per timestep. While EROW4 uses the augmented matrix approach to compute the φ function products,

EPIRK5P1BVAR takes a completely different approach to evaluating the ψ function products. It combines the Arnoldi process and the evaluation of ψ function products by sub-stepping, to make it adaptive, into a single computation process as described in [14].

Next we will discuss how we compute the ψ function products in the context of W -methods as they are closely related to classical methods in the computation of these products. Recall that W -methods admit arbitrary Jacobian approximations while maintaining full convergence order. In order to demonstrate this, we have alternate implementations that use different approximations to the Jacobian, namely, the Jacobian itself; the identity matrix; the zero matrix, which reduces the EPIRKW scheme (12) to an explicit Runge-Kutta scheme; and lastly, the diagonal of the Jacobian. We will refer to these methods as EPIRKW3 in the paper and highlight the approximation in the context. Figure 4 in the following section shows that these alternative implementations retain full order when we use an approximation to \mathbf{J}_n , as expected. It is to be noted, however, that in the case of W -methods, $\mathbf{A}_n = \mathbf{J}_n$ might be needed to assure stability, and some discussion in this regard when $\mathbf{A}_n = \mathbf{J}_n$ or when $\|\mathbf{A}_n - \mathbf{J}_n\|$ is small, is done in [7, Sec IV.7, IV.11] and [19].

The different implementations of the W -method vary in the way the ψ function products are computed. Among the many possible combinations, we will restrict our discussion of the evaluation of these products to the following cases:

1. $\mathbf{A}_n = \text{diag}(\mathbf{J}_n)$. We compute the individual φ_k functions with successively higher subscripts using the recursive definition given in (6), where φ_0 is computed as point-wise exponential of the entries along the diagonal. Next, we take the linear combination of the φ functions to evaluate the ψ function as defined in equation (9). Finally, the product of ψ function of matrix times vector is evaluated as a matrix-vector product. A similar procedure is adapted for other approximations where \mathbf{A}_n is either zero or identity.
2. $\mathbf{A}_n = \mathbf{J}_n$. The evaluation of products of ψ function of Jacobian with vectors is similar to the classical integrators. Three Arnoldi iterations are required for each new vector in the three stage formulation given in equation (12). An implementation involving a non-trivial approximation of the Jacobian may use a similar strategy to compute the ψ function products.

In addition to classical integrators and W -type integrators, we have implemented EPIRKK4, a fourth-order K -type integrator, and EPIRK5-K [21, Table 4], a classical fifth-order method implemented in the K -framework. These integrators use the reduced space formulation for stage values as shown in Algorithm 2. The reduced space is constructed using a single Arnoldi iteration per timestep. [26] proves that K -methods require only as many basis vectors in the reduced space as the order of the method to guarantee same order of convergence. This is in direct contrast to other methods considered in this paper that perform Arnoldi iteration where the basis size is variable and is dependent on the residual being below a chosen tolerance. EPIRKK4, being a fourth order K -method, theoretically requires only four vectors in the Krylov-subspace. Since the stage values of EPIRKK4 are computed in this reduced space, the size of the matrices used in the computation of ψ function products is usually smaller than the size of the ODE system under consideration. As a result, in our implementation of EPIRKK4, quantities $\varphi_k(h \gamma \mathbf{H})$ are directly computed using the recursive definition given in (6), they are stored independently and linearly combined to compute the ψ function. The product of a ψ function of a matrix with a vector is computed as a matrix-vector product. Despite using a similar procedure with five basis vectors in the Krylov-subspace, EPIRK5-K does not attain its theoretical order of convergence; the reason for this will become clear in the following section.

6. Numerical results

The integrators discussed in Section 5 were evaluated by running fixed-step convergence experiments on the Lorenz-96 system and variable time-stepping experiments on Lorenz-96, Shallow Water Equations, and Allen-Cahn system. In order to run variable time-stepping experiments, we used the MATLODE[®] framework [2], a MATLAB[®]-based ODE solver suite developed by the co-authors.

6.1. Lorenz-96 system

Lorenz-96 model [12] is described by the system of ODEs:

$$\frac{dy_j}{dt} = -y_{j-1}(y_{j-2} - y_{j+1}) - y_j + F, \quad j = 1 \dots N, \quad y_1 = y_N. \quad (30)$$

Here N denotes the number of states and F is the forcing term. For our experiments we let $N = 40$, and $F = 8$. The initial condition for the model was obtained by integrating over $[0, 0.3]$ time units using MATLAB's ODE45 integrator. Note also that the boundary condition is periodic.

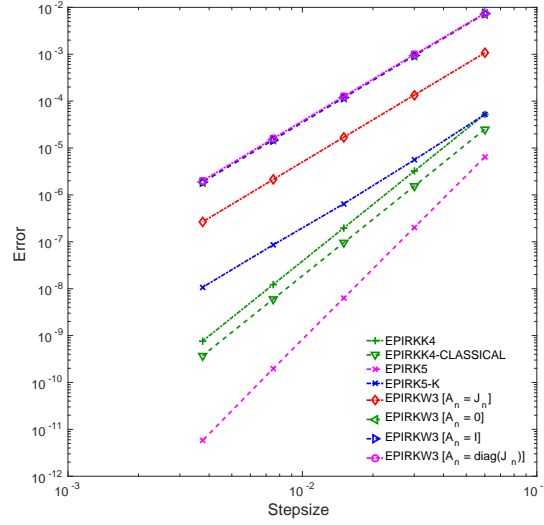


Figure 4: Convergence plot for different methods applied to Lorenz-96 model (30).

The Lorenz-96 system was used to perform fixed-step convergence experiments on a subset of integrators listed in Table 5. The reference solution was computed using ODE45 with absolute and relative tolerances set to $1e-12$. The convergence plots for fixed-step experiments are shown in Figure 4. The results for each implementation and coefficient combination are summarized in Table 5. These results support the following conclusions:

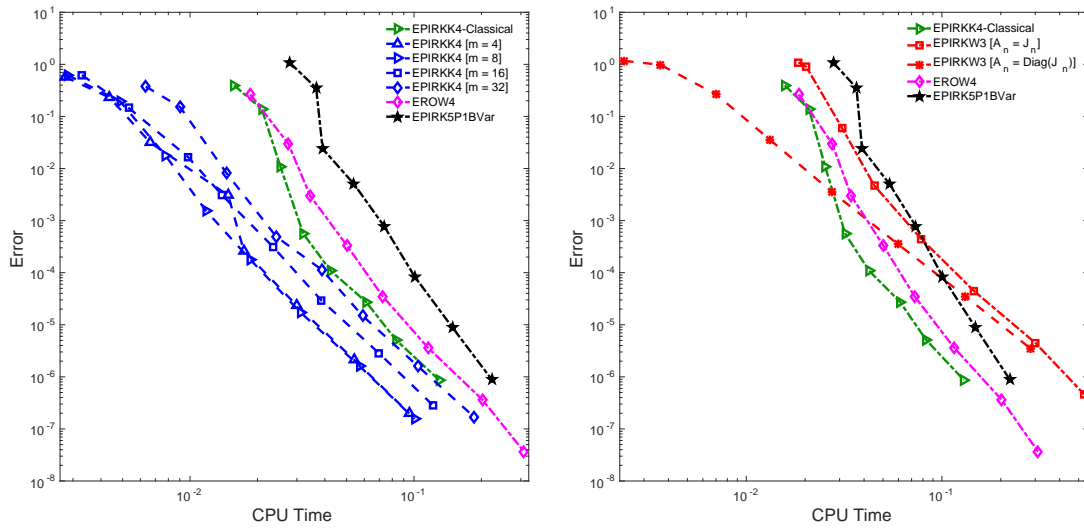
1. The numerical experiments verify the order of the methods derived in the paper. Both EPIRKK4 and EPIRKW3 show the theoretical order of convergence.
2. The theory of W -methods is validated through testing different approximations to the Jacobian. Indeed, EPIRKW3 consistently shows third order convergence irrespective of the approximation used for the Jacobian.
3. The results demonstrate that every K -method can be implemented as a classical method of the same order. Here we test EPIRKK4-CLASSICAL, the implementation of the method EPIRKK4 in the classical framework as discussed in Section 5. It has the same order of convergence as EPIRKK4 since the coefficients derived for EPIRKK4 method satisfies all the order conditions of a fourth order classical method. This is particularly true for every K -method.
4. In general, classical methods implemented as a K -methods do not preserve the order and may suffer from order reduction. Here EPIRK5 and EPIRK5-K were implemented for this specific purpose where EPIRK5-K is a K -type implementation of the fifth order classical method EPIRK5 derived in [21]. Clearly, from Table 5, we see that the K -type implementation shows order reduction as the coefficient

in front of the elementary differential corresponding to τ_8^K is non-zero in the K -type method. In general, solving the order conditions for a K -type method is more restrictive than solving for a classical method due to the additional order conditions that arise from approximating the Jacobian in the Krylov-subspace. As a result, not all classical methods lead to K -type integrators of the same order.

The last two observations are in line with Corollaries 4.6 and 4.7.

Integrator	Implementation Framework	Coefficients	Derived Order	Fixed Step Convergence Order
EPIRKK4	K -Type	Figure 3	4	4.018722
EPIRKK4-CLASSICAL	Classical	Figure 3	4	4.009777
\ddagger EPIRK5	Classical	[21, Table 4]	5	5.016092
\ddagger EPIRK5-K	K -Type	[21, Table 4]	5	3.051511
EPIRKW3 [$\mathbf{A}_n = \mathbf{J}_n$]	W -Type	Figure 2	3	2.994241
EPIRKW3 [$\mathbf{A}_n = \text{diag}(\mathbf{J}_n)$]	W -Type	Figure 2	3	2.967430
\ddagger EPIRKW3 [$\mathbf{A}_n = \mathbf{I}$]	W -Type	Figure 2	3	2.987911
\ddagger EPIRKW3 [$\mathbf{A}_n = \mathbf{0}$]	W -Type	Figure 2	3	2.977000
EROW4	Classical	[11, Section 5]	4	–
EPIRK5P1BVAR	Classical	[23, Table 3]	5	–

Table 5: Comparative study of various exponential integrators. The convergence orders shown are obtained from fixed step size experiments with the Lorenz-96 model (30). Integrators implemented only for studying fixed step convergence behavior are excluded from variable timestep experiments and these are prefixed with \ddagger in column 1.



(a) K-type versus classical methods

(b) W-type versus classical methods

Figure 5: Work-precision diagrams for different methods applied to Lorenz-96 problem (30).

To evaluate the relative computational efficiency of the integrators – EPIRKK4, EPIRKW3, and EPIRKK4-CLASSICAL – we perform variable time-stepping experiments with the Lorenz-96 system, the Shallow Water

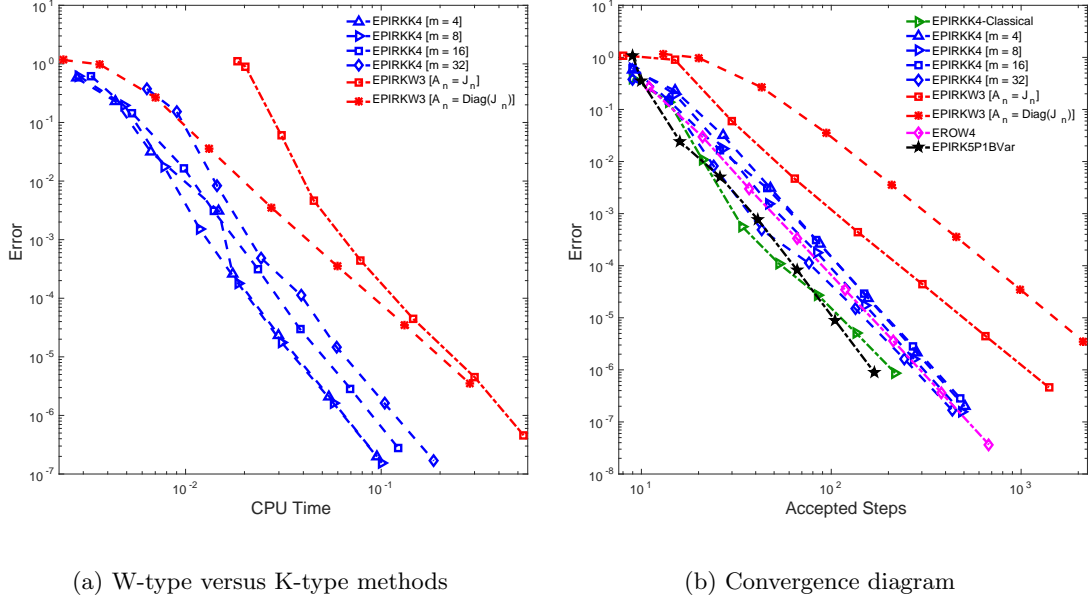


Figure 6: Work-precision and convergence diagrams for different methods applied to Lorenz-96 problem(30).

Equations, and the Allen-Cahn system. We also include known exponential schemes such as EPIRK5P1BVAR [23] and EROW4 [11, 22] as benchmark for the performance of the methods derived in this paper. Experiments are run for different relative tolerances $[1e-1, 1e-2, \dots, 1e-8]$; the error controller [6, Section II.4], which is the same across all methods, adjusts the stepsize to ensure that the solution meets the tolerance requirement. The relative tolerance for the Arnoldi algorithm was set to $1e-12$ for EPIRKK4, EPIRKK4-CLASSICAL and EROW4; $1e-9$ for EPIRKW3 ($\mathbf{A}_n = \mathbf{J}_n$) and to experimental tolerance for EPIRK5P1BVAR. As in the case of fixed-step convergence experiments, the reference solution is computed using ODE45 with absolute and relative tolerances equal to $1e-12$.

To aid the interpretation of the results, we organize the performance diagrams by subgroups of integrators. The work-precision diagrams for the Lorenz-96 system integrated over the time interval $[0, 1.8]$ [units], are shown in Figures 5a, 5b, and 6a. Figure 6b shows the convergence diagram for varying solution tolerances and plots the global error with respect to reference solution against the number of accepted steps. Table 6 reports the (root mean square) number of Krylov vectors used by each integrator per projection at each tolerance level. Table 7 gives the number of rejected time steps for each integrator at each tolerance level. Lastly, Table 8 interprets the global error at the end of the timespan and the timing results for each tolerance setting as the best CPU time in which certain level of accuracy is achieved by each integrator.

Figures 5a and 6a indicate that EPIRKK4 is more efficient than both EPIRKW3 ($\mathbf{A}_n = \mathbf{J}_n$) and the classical integrators on the Lorenz-96 system (30). This is because EPIRKK4 integrators use a single Krylov projection per timestep with a fixed number of basis vectors, not needing to compute any residuals along the way. On the other hand, each of the classical integrators and EPIRKW3 ($\mathbf{A}_n = \mathbf{J}_n$) need three Krylov projections per timestep and compute residuals to make Arnoldi adaptive. EPIRKK4-CLASSICAL, EROW4 and EPIRKW3 ($\mathbf{A}_n = \mathbf{J}_n$) build larger bases for high tolerance values, as can be seen from results reported in Table 6.

Between different fixed subspace sizes, EPIRKK4 with the basis size of four ($M = 4$) or eight ($M = 8$) performs better than those fixed at sixteen and thirty-two. The increased cost of performing Arnoldi for larger basis sizes does not give a proportionate advantage in terms of stability as all the EPIRKK4 runs end up taking approximately the same number of timesteps as indicated in Figure 6b. However, runs with larger basis size do more work per timestep.

Integrator \ Tolerance	10^{-1}	10^{-2}	10^{-3}	10^{-4}	10^{-5}	10^{-6}	10^{-7}	10^{-8}
EPIRKK4-CLASSICAL	18	16	13	12	10	9	7	7
EPIRKK4 [M = 4]	4	4	4	4	4	4	4	4
EPIRKK4 [M = 8]	8	8	8	8	8	8	8	8
EPIRKK4 [M = 16]	16	16	16	16	16	16	1	16
EPIRKK4 [M = 32]	32	32	32	32	32	32	32	32
EPIRKW3 [$\mathbf{A}_n = \mathbf{J}_n$]	20	14	10	7	6	5	4	3
EPIRKW3 [$\mathbf{A}_n = \text{diag}(\mathbf{J}_n)$]	0	0	0	0	0	0	0	0
EROW4	20	15	12	10	8	7	7	5
EPIRK5P1BVAR	13	8	6	5	5	4	4	4

Table 6: Root mean square number of Krylov vectors per projection for each integrator applied to Lorenz-96 problem (30). EPIRKK4 uses a fixed number of basis vectors in the Arnoldi process (indicated by the value m in brackets). EPIRKW3 with $\mathbf{A}_n = \text{diag}(\mathbf{J}_n)$ computes the ψ function product directly, without the need to perform Arnoldi. Both EPIRKW3 with $\mathbf{A}_n = \mathbf{J}_n$ and the classical methods use an adaptive Arnoldi process to approximate the ψ function product.

Integrator \ Tolerance	10^{-1}	10^{-2}	10^{-3}	10^{-4}	10^{-5}	10^{-6}	10^{-7}	10^{-8}
EPIRKK4-CLASSICAL	5	6	7	5	4	1	0	0
EPIRKK4 [M = 4]	5	7	6	5	3	1	0	0
EPIRKK4 [M = 8]	4	7	9	8	2	0	0	0
EPIRKK4 [M = 16]	3	5	9	6	5	0	0	0
EPIRKK4 [M = 32]	5	5	8	11	12	3	0	0
EPIRKW3 [$\mathbf{A}_n = \mathbf{J}_n$]	6	6	9	7	0	0	0	0
EPIRKW3 [$\mathbf{A}_n = \text{diag}(\mathbf{J}_n)$]	5	6	9	2	0	0	0	0
EROW4	4	7	6	6	1	0	0	0
EPIRK5P1BVAR	5	4	5	7	4	4	1	0

Table 7: Total number of rejected timesteps for each integrator applied to Lorenz-96 problem (30). EPIRKK4 [M = 32] attempts to take large steps in the high tolerance region, but the stepsize controller rejects them and forces it to take about the same number of steps as other methods.

Integrator \ Accuracy	10^{-1}	10^{-2}	10^{-3}	10^{-4}	10^{-5}	10^{-6}	10^{-7}
EPIRKK4-CLASSICAL	.025	—	.032	.061	.083	.129	—
EPIRKK4 [M = 4]	.007	.015	.017	.03	.054	.095	—
EPIRKK4 [M = 8]	.008	.012	.019	.031	.057	.101	—
EPIRKK4 [M = 16]	.01	.014	.023	.039	.07	.122	—
EPIRKK4 [M = 32]	—	.015	.024	.059	.104	.186	—
EPIRKW3 [$\mathbf{A}_n = \mathbf{J}_n$]	.031	.045	.078	.146	.301	.535	—
EPIRKW3 [$\mathbf{A}_n = \text{diag}(\mathbf{J}_n)$]	.013	.027	.06	.132	.283	—	—
EROW4	.027	.034	.05	.073	.116	.202	.31
EPIRK5P1BVAR	.039	.054	.074	.101	.149	.223	—

Table 8: CPU time in which accuracy is achieved by different integrators applied to Lorenz-96 problem (30).

The difference in performance between the classical integrators can be attributed to the way the computation of ψ function products is carried out. EPIRKK4-CLASSICAL and EROW4 use the augmented matrix approach described in Section 5 and only compute the residual at specific indices, where the cost of computing the residual equals the total cost of computing the basis vectors up to that point [9, Section 6.4]. On the other hand, EPIRK5P1BVAR computes the ψ function product according to [14], which involves sub-stepping and other complex arithmetic operations that do not pay off in the case of Lorenz-96 system.

As seen in Figure 5b, EPIRKW3 ($\mathbf{A}_n = \mathbf{J}_n$) behaves like a classical exponential method. The implementation uses three Krylov projections per timestep and does mathematical operations involving matrices of approximately the same size as classical exponential methods, except it only has third order convergence. As a consequence, its performance is similar to that of classical exponential methods in the low-to-medium accuracy regime. In the medium-to-high accuracy regime the performance is less competitive, and Figure 6b shows that this is due to the many more steps taken by the integrator EPIRKW3 ($\mathbf{A}_n = \mathbf{J}_n$), as enforced by the stepsize controller.

In contrast, EPIRKW3 ($\mathbf{A}_n = \text{diag}(\mathbf{J}_n)$) does not need any Arnoldi iterations. Moreover, computations do not involve operations on large matrices. This makes EPIRKW3 ($\mathbf{A}_n = \text{diag}(\mathbf{J}_n)$) very inexpensive per timestep. Even though the method appears to be efficient for low accuracy solutions, relative error in the region is $\mathcal{O}(1)$ as is for all other methods. For medium-to-high accuracy solutions, the method takes significantly more number of timesteps, as is shown in Figure 6b, explaining the tilt towards higher CPU time. In the case of EPIRKW3 ($\mathbf{A}_n = \text{diag}(\mathbf{J}_n)$), we note that the larger number of timesteps for high accuracy solutions is due to a combination of lower order of the W -method and insufficient stability as the approximation to the exact Jacobian is not fully representative of its structure. Good Jacobian approximations for the problem at hand are important in order to take full advantage of the capabilities of EPIRK- W methods.

6.2. Shallow water equations on the sphere

The Shallow Water Equations (SWE) on the sphere [5, 13, 16] are given by:

$$\begin{aligned} \frac{\partial u}{\partial t} + \frac{1}{a \cos \theta} \left[u \frac{\partial u}{\partial \lambda} + v \cos \theta \frac{\partial u}{\partial \theta} \right] - \left(f + \frac{u}{a} \tan \theta \right) v + \frac{g}{a \cos \theta} \frac{\partial h}{\partial \lambda} &= 0, \\ \frac{\partial v}{\partial t} + \frac{1}{a \cos \theta} \left[u \frac{\partial v}{\partial \lambda} + v \cos \theta \frac{\partial v}{\partial \theta} \right] + \left(f + \frac{u}{a} \tan \theta \right) u + \frac{g}{a} \frac{\partial h}{\partial \theta} &= 0, \\ \frac{\partial h}{\partial t} + \frac{1}{a \cos \theta} \left[\frac{\partial(hu)}{\partial \lambda} + \frac{\partial(hv \cos \theta)}{\partial \theta} \right] &= 0, \end{aligned} \quad (31)$$

where f is the Coriolis parameter given by $f = 2\Omega \sin \theta$, with Ω being the angular speed of the rotation of the earth, h is the height of the atmosphere, u and v are zonal and meridional wind components, a is the radius of the earth and g is the gravitational constant, θ and λ are latitudinal and longitudinal directions respectively. Initial conditions for the shallow water equations are same as those that appear in [13, Section 6]. The model was discretized in space with 72 gridpoints along each latitude and 36 gridpoints along each longitude. The system has three variables, u , v and h , that need to be computed at each grid point making the total dimension of the semi-discrete system $N = 7776$.

We ran variable time-stepping experiments on the shallow water equations model over the integration window $[0, 28800]$ time units, which roughly corresponds to one day of real time. The work precision diagrams appear in Figures 7a, 7b, and 8a. Figure 8b is the convergence diagram for varying solution tolerances and plots the global error with respect to reference solution against the number of accepted steps. Table 9 details the (root mean square) number of Krylov vectors per projection used by each integrator at each tolerance level. Table 10 specifies the number of rejected timesteps for each integrator at each tolerance level.

Figure 7a suggests that for the Shallow Water Equations on sphere problem, EPIRKK4 with basis size set to eight (sixteen) is able to achieve solutions in the high tolerance region unlike the classical integrators, and in appropriately less amount of time. EPIRKK4 with sixteen basis vectors continues to be atleast 23% more efficient until a solution accuracy of $1e-5$ before becoming slightly more expensive than the classical

Integrator \ Tolerance	10^{-1}	10^{-2}	10^{-3}	10^{-4}	10^{-5}	10^{-6}	10^{-7}	10^{-8}
EPIRKK4-CLASSICAL	25	25	25	27	26	21	16	12
EPIRKK4 [M = 4]	4	4	4	4	4	4	4	4
EPIRKK4 [M = 8]	8	8	8	8	8	8	8	8
EPIRKK4 [M = 16]	16	16	16	16	16	16	16	16
EPIRKK4 [M = 32]	32	32	32	32	32	32	32	32
EPIRKW3 [$\mathbf{A}_n = \mathbf{J}_n$]	21	21	21	20	14	8	5	4
EROW4	30	30	22	22	16	12	8	7
EPIRK5P1BVAR	57	53	38	30	23	19	16	14

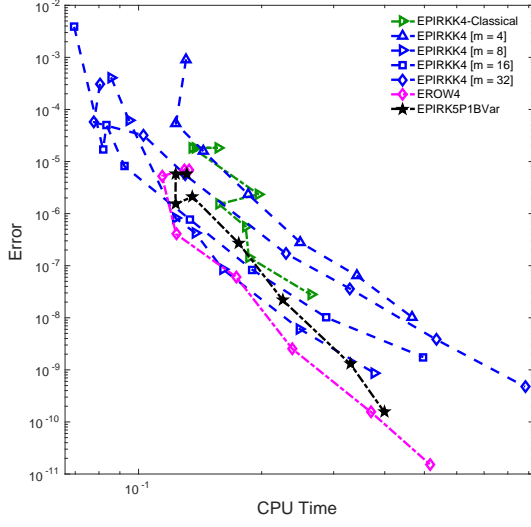
Table 9: Root mean square number of Krylov vectors per projection for each integrator applied to Shallow Water Equations problem (31). EPIRKK4 uses fixed number of basis vectors in the Arnoldi process as indicated in brackets succeeding the name of the method. EPIRKW3 with $A_n = \text{diag}(J_n)$ directly computes the ψ function product not needing to perform Arnoldi. All other methods, both EPIRKW3 with $A_n = J_n$ and the classical methods use an adaptive Arnoldi process to approximate the ψ function product.

Integrator \ Tolerance	10^{-1}	10^{-2}	10^{-3}	10^{-4}	10^{-5}	10^{-6}	10^{-7}	10^{-8}
EPIRKK4-CLASSICAL	0	0	0	2	1	2	2	4
EPIRKK4 [M = 4]	12	6	7	5	8	11	13	10
EPIRKK4 [M = 8]	15	3	3	6	6	6	7	6
EPIRKK4 [M = 16]	3	2	2	2	4	6	7	18
EPIRKK4 [M = 32]	1	0	1	2	6	7	9	16
EPIRKW3 [$\mathbf{A}_n = \mathbf{J}_n$]	0	0	0	1	3	3	7	2
EROW4	0	0	1	0	3	6	9	8
EPIRK5P1BVAR	0	0	0	0	1	2	6	5

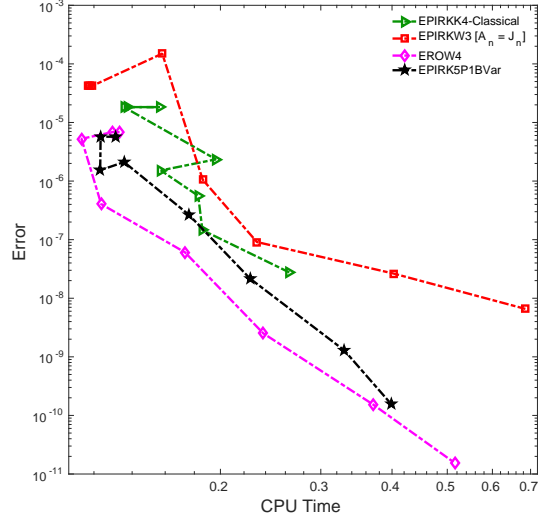
Table 10: Total number of rejected timesteps for each integrator applied to Shallow Water Equations problem (31).

Integrator \ Accuracy	10^{-2}	10^{-3}	10^{-4}	10^{-5}	10^{-6}	10^{-7}	10^{-8}	10^{-9}
EPIRKK4-CLASSICAL	—	—	.135	.157	.183	.264	—	—
EPIRKK4 [M = 4]	—	.131	.123	.185	.249	.342	—	—
EPIRKK4 [M = 8]	—	.086	.095	—	.123	.161	.247	.378
EPIRKK4 [M = 16]	.07	—	.082	.092	.134	.19	.497	—
EPIRKK4 [M = 32]	—	.08	.078	.13	.23	.329	.534	.882
EPIRKW3 [$\mathbf{A}_n = \mathbf{J}_n$]	—	.158	.117	.186	—	.232	.685	—
EROW4	—	—	—	.114	.124	.173	.238	.37
EPIRK5P1BVAR	—	—	—	.123	.176	.225	.33	.399

Table 11: CPU time in which accuracy is achieved by different integrators applied to Shallow Water Equations problem (31). In our experiments, only EROW4 achieves an accuracy of $1e-10$ in 0.515 seconds.

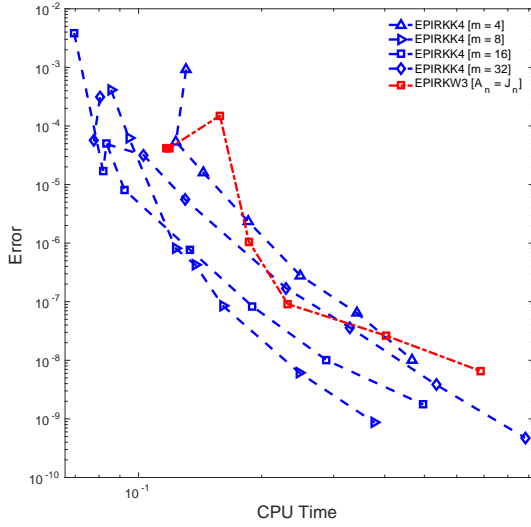


(a) K-type versus classical methods

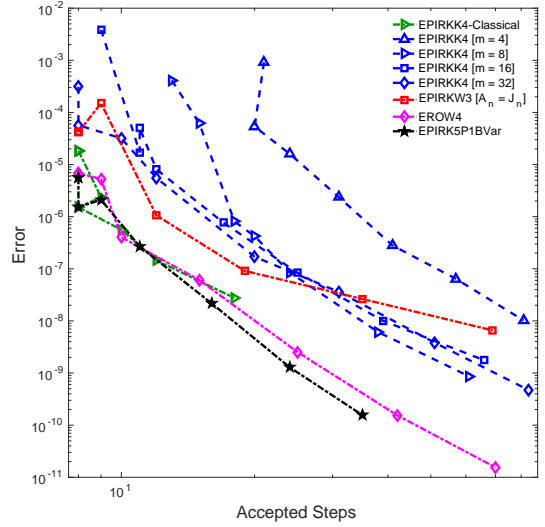


(b) W-type versus classical methods

Figure 7: Work-precision diagrams for different methods applied to Shallow Water Equations problem (31).



(a) W-type versus K-type methods



(b) Convergence diagram

Figure 8: Work-precision and convergence diagrams for different methods applied to Shallow Water Equations problem (31).

methods. On the other hand, EPIRKK4 with basis size eight remains to be about as good as the classical methods for the entire tolerance spectrum. It is rather interesting that increasing the basis size to sixteen or thirty-two does not significantly improve the performance of EPIRKK4 integrators and in some cases makes

them perform poorly. This can be explained based on Figure 8b where executions with eight, sixteen and thirty-two basis vectors end up taking approximately the same number of timesteps beyond a tolerance setting of $1e-6$ making executions with larger basis size cost more per timestep. For these runs of EPIRKK4, attempts to increase the stepsize are faced with step rejections as shown in Table 10.

Among different executions of EPIRKK4, one with four basis vectors performs the poorest as seen in Figure 7a and 8a. This is because four basis vectors in the Krylov-subspace is insufficient to capture the dynamics of the ODE system under consideration forcing the integrator to take significantly more timesteps than other executions of EPIRKK4 (see Figure 8b).

EPIRKW3 method with $\mathbf{A}_n = \mathbf{J}_n$ performs like classical exponential integrators as shown in Figure 7b and this is explained in Section 6.1. We notice that the error controller forces the method to take larger number of time steps as accuracy increases (see Figure 8b) explaining the deviation from the classical integrators for lower tolerances.

For the Shallow Water Equation system, EPIRKW3 with $\mathbf{A}_n = \text{diag}(\mathbf{J}_n)$ did not converge for any tolerance setting as the method was highly unstable. This can be explained by the structure of the exact Jacobian versus that of the approximate Jacobian. The exact Jacobian is not diagonally dominant and has an incomplete banded structure. On the other hand, the approximation only includes the diagonal and is diagonally dominant. Therefore, we exclude EPIRKW3 with $\mathbf{A}_n = \text{diag}(\mathbf{J}_n)$ from our current discussion.

Table 11 presents an alternative approach to interpreting the work precision diagrams. It shows the best CPU time by which each integrator could achieve a certain level of accuracy.

6.3. The Allen-Cahn problem

We consider the Allen-Cahn equation [1]:

$$\frac{\partial u}{\partial t} = \alpha \nabla^2 u + \gamma (u - u^3), \quad (x, y) \in [0, 1] \times [0, 1] \text{ (space units)}, \quad t \in [0, 1.2] \text{ (time units)}. \quad (32)$$

For our experiments we set $\alpha = 0.01$ and $\gamma = 1.0$. The model has homogeneous Neumann boundary conditions and the initial conditions are $u(t=0) = 0.4 + 0.1(x+y) + 0.1 \sin(10x) \sin(20y)$. Discretization is done in the spatial domain using finite difference for two different grid sizes – 64×64 and 256×256 . The work-precision diagrams from variable time-stepping are shown in Figures 9a, 9b, and 10a for grid of size 64×64 . Figure 10b shows the corresponding convergence diagram and plots the global error with respect to the reference against the number of accepted steps. Table 12 shows the (root mean square) number of Krylov vectors per projection used by each method at different tolerance levels. Table 14 is a reinterpretation of the work precision diagrams in a tabular form where each entry represents the best CPU time in which the solution at the end of the timespan attains a certain level of accuracy. Figures 11a, 11b, 12a and 12b, and Tables 15, 16 and 17 correspond to results from performing the same experiment on a grid of size 256×256 .

Figure 9a demonstrates that EPIRKK4 with basis size set to either sixteen ($m = 16$) or thirty-two ($m = 32$) is more efficient than classical exponential methods for the Allen-Cahn problem (32) on a spatial grid of size 64×64 . EPIRKK4 with basis size four requires a large number of timesteps relative to both classical and EPIRKK4 executions with larger basis sizes, as shown in Figure 10b. It also suffers from step rejections as indicated in Table 13. As a consequence, despite being very cheap per timestep, EPIRKK4 performs the poorest among all EPIRKK4 executions.

As the tolerance is tightened, all integrators, barring a few, are forced to take small steps that are approximately of the same size as seen in Figure 10b. As a consequence, integrators that are cheap per timestep are more efficient for high accuracy solutions. EPIRKK4 with eight basis vectors ($m = 8$) comes out on top in this regard.

EPIRKW3 with $\mathbf{A}_n = \mathbf{J}_n$ behaves like a classical method, but takes more steps in the high accuracy region due to its lower order, as shown in Figure 10b. The same figure illustrates that EPIRKW3 with $\mathbf{A}_n = \text{diag}(\mathbf{J}_n)$ takes significantly more steps than all other integrators and also suffers from step rejections in the low accuracy region (Table 13). Both step rejection and small step size contribute to a poor performing integrator in its case.

As the grid resolution is increased to 256×256 , the picture is similar with some notable exceptions (see Figures 11a, 12a and 12b). EPIRKK4 with basis size set to sixteen is no longer performing as well

Integrator \ Tolerance	10^{-1}	10^{-2}	10^{-3}	10^{-4}	10^{-5}	10^{-6}	10^{-7}	10^{-8}
EPIRKK4-CLASSICAL	49	49	42	37	30	23	19	16
EPIRKK4 [M = 4]	4	4	4	4	4	4	4	4
EPIRKK4 [M = 8]	8	8	8	8	8	8	8	8
EPIRKK4 [M = 16]	16	16	16	16	16	16	16	16
EPIRKK4 [M = 32]	32	32	32	32	32	32	32	32
EPIRKW3 [$\mathbf{A}_n = \mathbf{J}_n$]	48	48	37	26	17	11	7	5
EPIRKW3 [$\mathbf{A}_n = \text{diag}(\mathbf{J}_n)$]	0	0	0	0	0	0	0	0
EROW4	57	57	47	39	29	21	15	12
EPIRK5P1BVAR	32	47	52	43	31	21	18	15

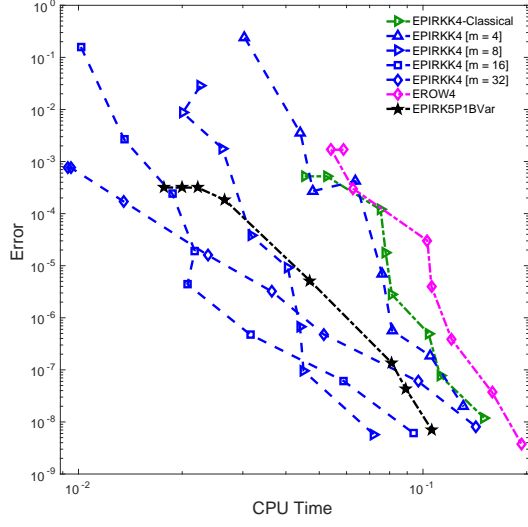
Table 12: Root mean square number of Krylov vectors per projection for each integrator applied to Allen-Cahn problem (32) on a 64×64 grid. EPIRKK4 uses fixed number of basis vectors in the Arnoldi process as indicated in brackets succeeding the name of the method. EPIRKW3 with $\mathbf{A}_n = \text{diag}(\mathbf{J}_n)$ directly computes the ψ function product not needing to perform Arnoldi. All other methods, both EPIRKW3 with $\mathbf{A}_n = \mathbf{J}_n$ and the classical methods use an adaptive Arnoldi process to approximate the ψ function product.

Integrator \ Tolerance	10^{-1}	10^{-2}	10^{-3}	10^{-4}	10^{-5}	10^{-6}	10^{-7}	10^{-8}
EPIRKK4-CLASSICAL	0	0	1	0	0	1	0	0
EPIRKK4 [M = 4]	4	2	2	11	3	6	14	8
EPIRKK4 [M = 8]	6	1	1	3	6	5	0	0
EPIRKK4 [M = 16]	1	1	2	2	0	0	0	0
EPIRKK4 [M = 32]	0	0	0	0	0	0	0	0
EPIRKW3 [$\mathbf{A}_n = \mathbf{J}_n$]	0	0	0	0	0	0	0	0
EPIRKW3 [$\mathbf{A}_n = \text{diag}(\mathbf{J}_n)$]	0	15	15	13	11	0	0	0
EROW4	0	0	0	1	0	0	0	0
EPIRK5P1BVAR	0	0	0	0	0	1	0	0

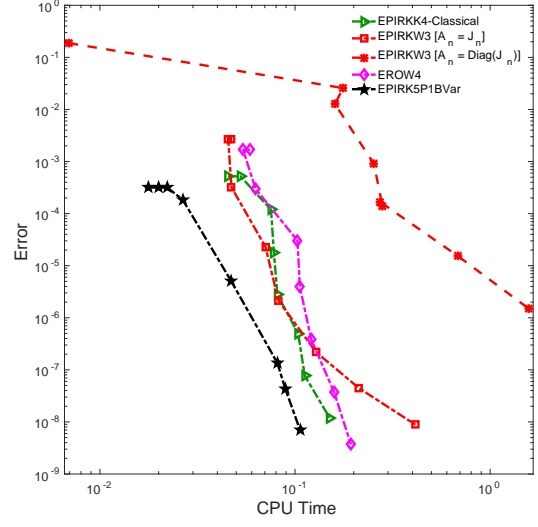
Table 13: Total number of rejected timesteps for each integrator applied to Allen-Cahn problem (32) on a 64×64 grid. EPIRKK4 executions with basis sizes set to four or eight suffer from step rejections and take large number of timesteps for all different tolerance levels. EPIRKW3 with $\mathbf{A}_n = \text{diag}(\mathbf{J}_n)$ also shows similar behavior. This hints at the poor stability of these methods.

Integrator \ Accuracy	10^{-1}	10^{-2}	10^{-3}	10^{-4}	10^{-5}	10^{-6}	10^{-7}	10^{-8}
EPIRKK4-CLASSICAL	—	—	.045	.078	.081	.104	.112	—
EPIRKK4 [M = 4]	—	.044	.048	—	.076	.081	.131	—
EPIRKK4 [M = 8]	.023	.02	—	.032	.041	.044	.045	.072
EPIRKK4 [M = 16]	—	.014	.019	.022	.021	.032	.059	.094
EPIRKK4 [M = 32]	—	—	.009	.024	.036	.052	.097	.143
EPIRKW3 [$\mathbf{A}_n = \mathbf{J}_n$]	—	.045	.047	.071	.082	.128	.212	.414
EPIRKW3 [$\mathbf{A}_n = \text{diag}(\mathbf{J}_n)$]	.16	—	.254	.683	1.583	—	—	—
EROW4	—	.054	.063	.103	.106	.121	.159	.193
EPIRK5P1BVAR	—	—	.018	—	.047	.081	.089	.106

Table 14: CPU time in which accuracy is achieved by different integrators applied to Allen-Cahn problem (32) on a 64×64 grid.

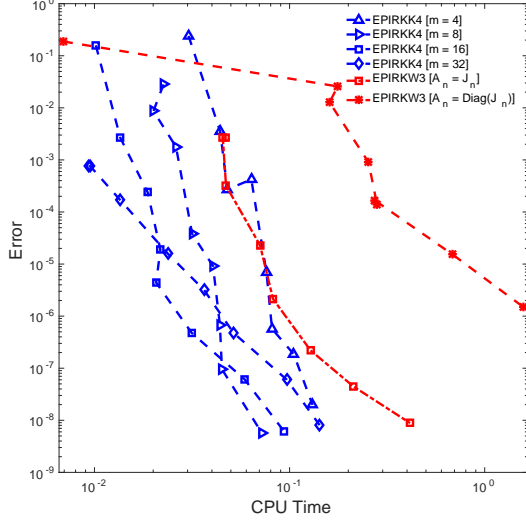


(a) K-type versus classical methods

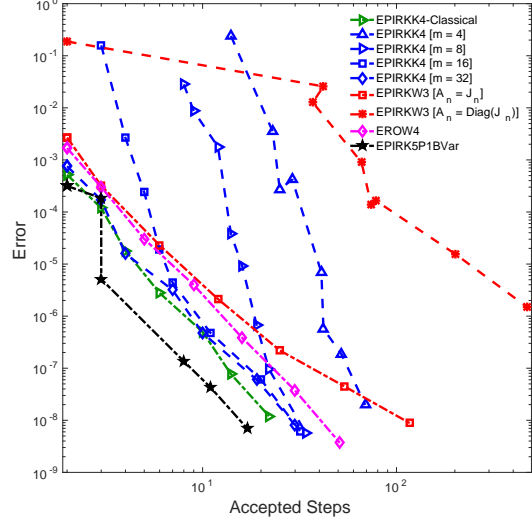


(b) W-type versus classical methods

Figure 9: Work-precision diagrams for different methods applied to Allen-Cahn problem (32) on a 64×64 grid.



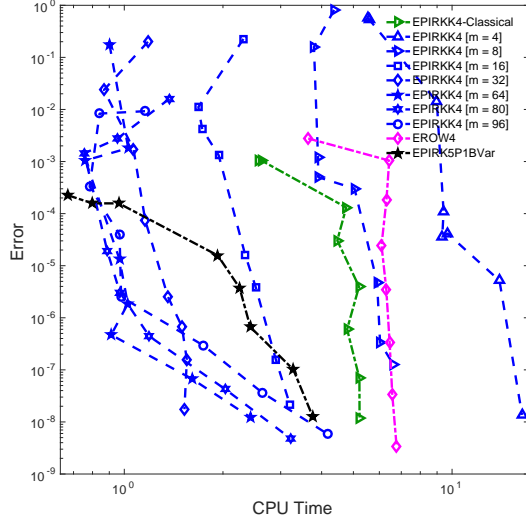
(a) W-type versus K-type methods



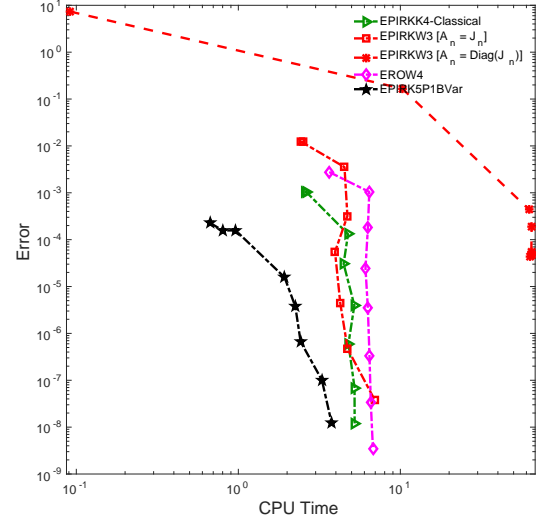
(b) Convergence diagram

Figure 10: Work-precision diagrams and convergence diagrams for different methods applied to Allen-Cahn problem (32) on a 64×64 grid.

as before. Larger basis sizes are required to gain enough stability while remaining cheap per timestep. Although choosing the basis size adaptively for K -methods seems to be a natural next step, this has not

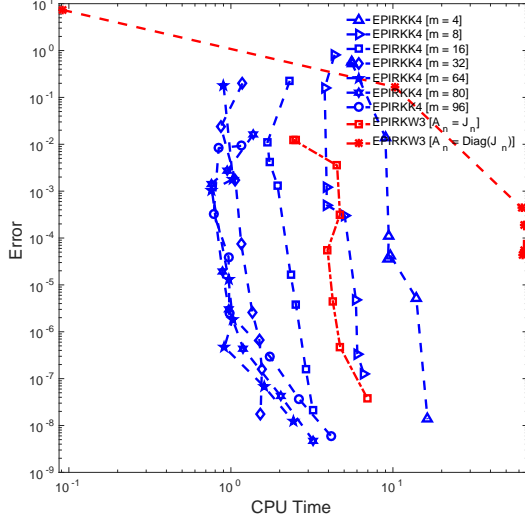


(a) K-type versus classical methods

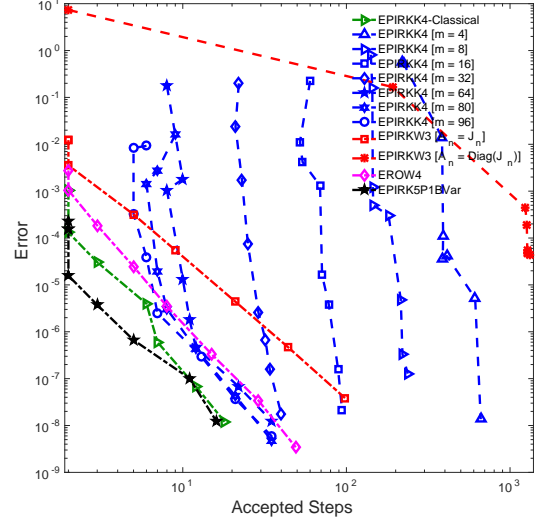


(b) W-type versus classical methods

Figure 11: Work-precision diagrams for different methods applied to Allen-Cahn problem (32) on a 256×256 grid.



(a) W-type versus K-type methods



(b) Convergence diagram

Figure 12: Work-precision diagrams and convergence diagrams for different methods applied to Allen-Cahn problem (32) on a 256×256 grid.

been investigated as part of current work and will be considered as future extension.

Tables 14 and 17 summarize the results of the work precision diagrams in a tabular fashion where

Integrator \ Tolerance	10^{-1}	10^{-2}	10^{-3}	10^{-4}	10^{-5}	10^{-6}	10^{-7}	10^{-8}
EPIRKK4-CLASSICAL	192	192	211	177	131	118	92	75
EPIRKK4 [M = 4]	4	4	4	4	4	4	4	4
EPIRKK4 [M = 8]	8	8	8	8	8	8	8	8
EPIRKK4 [M = 16]	16	16	16	16	16	16	16	16
EPIRKK4 [M = 32]	32	32	32	32	32	32	32	32
EPIRKK4 [M = 64]	64	64	64	64	64	64	64	64
EPIRKK4 [M = 80]	80	80	80	80	80	80	80	80
EPIRKK4 [M = 96]	96	96	96	96	96	96	96	96
EPIRKW3 [$\mathbf{A}_n = \mathbf{J}_n$]	186	186	204	125	93	61	41	28
EPIRKW3 [$\mathbf{A}_n = \text{diag}(\mathbf{J}_n)$]	0	0	0	0	0	0	0	0
EROW4	231	254	215	170	133	100	71	54
EPIRK5P1BVAR	328	358	410	475	420	331	234	205

Table 15: Root mean square number of Krylov vectors per projection for each integrator applied to Allen-Cahn problem (32) on a 256×256 grid. EPIRKK4 uses fixed number of basis vectors in the Arnoldi process as indicated in brackets succeeding the name of the method. EPIRKW3 with $\mathbf{A}_n = \text{diag}(\mathbf{J}_n)$ directly computes the ψ function product not needing to perform Arnoldi. All other methods, both EPIRKW3 with $\mathbf{A}_n = \mathbf{J}_n$ and the classical methods use an adaptive Arnoldi process to approximate the ψ function product.

Integrator \ Tolerance	10^{-1}	10^{-2}	10^{-3}	10^{-4}	10^{-5}	10^{-6}	10^{-7}	10^{-8}
EPIRKK4-CLASSICAL	0	0	0	0	1	1	1	1
EPIRKK4 [M = 4]	76	70	36	77	80	53	8	168
EPIRKK4 [M = 8]	110	36	49	46	81	84	87	106
EPIRKK4 [M = 16]	56	24	22	6	37	36	43	49
EPIRKK4 [M = 32]	16	3	10	11	13	14	14	1
EPIRKK4 [M = 64]	5	5	3	4	4	0	0	0
EPIRKK4 [M = 80]	6	4	2	2	2	0	0	0
EPIRKK4 [M = 96]	3	2	1	2	0	0	0	0
EPIRKW3 [$\mathbf{A}_n = \mathbf{J}_n$]	0	0	0	2	1	1	0	0
EPIRKW3 [$\mathbf{A}_n = \text{diag}(\mathbf{J}_n)$]	0	46	156	181	169	169	164	41
EROW4	0	0	0	0	0	0	0	0
EPIRK5P1BVAR	0	0	0	0	0	0	0	0

Table 16: Total number of rejected timesteps for each integrator applied to Allen-Cahn problem (32) on a 256×256 grid. EPIRKK4 executions with smaller basis sizes suffer severely from step rejections and take large number of timesteps for all different tolerance levels and so does EPIRKW3 with $\mathbf{A}_n = \text{diag}(\mathbf{J}_n)$, signaling the poor stability of these methods.

they show the best CPU time in which the integrators attain certain prescribed levels of accuracy for the Allen-Cahn problem (32) on a 64×64 and 256×256 grid, respectively.

We also performed additional experiments with variable time stepping on the Allen-Cahn problem (32) (64×64 grid) for different time spans ranging between $[0, 0.2]$ units to $[0, 9.6]$ units. Those results are not reported here in detail. We noticed that the relative performance of the classical methods and K -methods depends on the time span: in some instances the classical methods perform as well as the K -methods, while in other instances they perform more poorly than for the cases shown in the paper. We could not conclusively point to the cause of this variability in the relative performance.

Integrator \ Accuracy	10^{-1}	10^{-2}	10^{-3}	10^{-4}	10^{-5}	10^{-6}	10^{-7}	10^{-8}
EPIRKK4-CLASSICAL	—	2.567	4.754	4.465	5.201	4.784	5.216	—
EPIRKK4 [M = 4]	8.984	—	9.422	9.333	13.949	—	16.353	—
EPIRKK4 [M = 8]	—	3.899	3.903	—	5.907	6.03	—	—
EPIRKK4 [M = 16]	1.683	1.729	—	2.337	2.518	2.901	3.202	—
EPIRKK4 [M = 32]	.867	1.067	—	1.158	1.357	1.499	1.526	—
EPIRKK4 [M = 64]	—	.761	—	.967	1.025	.912	1.609	—
EPIRKK4 [M = 80]	1.373	.755	—	.888	.97	1.192	2.033	3.222
EPIRKK4 [M = 96]	—	.841	.784	.967	.978	1.742	2.635	4.172
EPIRKW3 [$\mathbf{A}_n = \mathbf{J}_n$]	2.444	4.522	4.712	3.952	4.26	4.727	6.932	—
EPIRKW3 [$\mathbf{A}_n = \text{diag}(\mathbf{J}_n)$]	—	—	62.205	62.858	—	—	—	—
EROW4	—	3.641	6.308	6.093	6.3	6.45	6.57	6.772
EPIRK5P1BVAR	—	—	.672	1.928	2.248	2.423	3.76	—

Table 17: CPU time in which accuracy is achieved by different integrators applied to Allen-Cahn problem (32) on a 256×256 grid.

7. Conclusions

Exponential Propagation Iterative Methods of Runge-Kutta type (EPIRK) rely on the computation of exponential-like matrix functions of the Jacobian times vector products. This paper develops two new classes of EPIRK methods that allow the use of inexact Jacobians as arguments of the matrix functions. We derive a general order conditions theory for EPIRK- W -methods, which admit arbitrary approximations of the Jacobian, and for EPIRK- K -methods, which use a specific Krylov-subspace based approximation of the Jacobian. We also provide a computational procedure to derive order conditions for methods with an arbitrary number of stages, and solve the order conditions of a three stage formulation to obtain coefficients for two third order EPIRK- W -methods, named EPIRKW3, and a fourth order EPIRK- K -method, named EPIRKK4. Several alternative implementations of W -methods and K -methods are discussed, and their properties are studied.

Numerical experiments are conducted with three different test problems to study the performance of the new methods. The results confirm empirically that EPIRKW3-method retains third order of convergence with different Jacobian approximations. The EPIRKK4-method is computationally more efficient than EPIRKW3 and performs better than classical methods in a number of different scenarios considered in the paper. In particular EPIRKK4 outperforms EPIRKK4-CLASSICAL, a method with the same set of coefficients, but implemented in the classical framework for exponential integrators. More numerical experiments are needed to asses how these results generalize to different applications.

It was also observed that increasing the basis size can make EPIRKK4 more stable, but there is a cost to pay for it and that it is important to balance gains in stability against the increased computational cost. An adaptive approach to basis size selection for the K -methods is relevant in this regard and will be considered in future work.

Acknowledgements

This work has been supported in part by NSF through awards NSF DMS-1419003, NSF DMS-1419105, NSF CCF-1613905, AFOSR FA9550-12-1-0293-DEF, and by the Computational Science Laboratory at Virginia Tech.

A. Derivation of K -methods

The EPIRKK method is derived from EPIRKW method, where a specific Krylov-subspace approximation of the Jacobian is used instead of an arbitrary approximate Jacobian as admitted by the W -method. We

start the derivation by first stating the general form of the EPIRKW method:

$$Y_i = y_n + a_{i,1} \psi_{i,1}(g_{i,1} h \mathbf{A}_n) h f(y_n) + \sum_{j=2}^i a_{i,j} \psi_{i,j}(g_{i,j} h \mathbf{A}_n) h \Delta^{(j-1)} r(y_n), \quad i = 1, \dots, s-1,$$

$$y_{n+1} = y_n + b_1 \psi_{s,1}(g_{s,1} h \mathbf{A}_n) h f(y_n) + \sum_{j=2}^s b_j \psi_{s,j}(g_{s,j} h \mathbf{A}_n) h \Delta^{(j-1)} r(y_n).$$

In the above equation, the ψ function is as defined in equation (8) and the following simplifying assumption is made about it:

$$\psi_{i,j}(z) = \psi_j(z) = \sum_{k=1}^j p_{j,k} \varphi_k(z),$$

where φ function is as defined in equation (5), (6). Additionally, the remainder function ($r(y)$) and the forward difference operator ($\Delta^{(j)} r(Y_i)$) are defined accordingly below:

$$\begin{aligned} r(y) &= f(y) - f(y_n) - \mathbf{A}_n (y - y_n), \\ \Delta^{(j)} r(Y_i) &= \Delta^{(j-1)} r(Y_{i+1}) - \Delta^{(j-1)} r(Y_i), \\ \Delta^{(1)} r(Y_i) &= r(Y_{i+1}) - r(Y_i). \end{aligned} \tag{A.1}$$

The K -method uses a specific Krylov-subspace based approximation of the Jacobian (\mathbf{J}_n). An M -dimensional Krylov-subspace is built as,

$$\mathcal{K}_M = \text{span}\{f_n, \mathbf{J}_n f_n, \mathbf{J}_n^2 f_n, \dots, \mathbf{J}_n^{M-1} f_n\}, \tag{A.2}$$

whose basis is the orthonormal matrix \mathbf{V} and \mathbf{H} is the upper-Hessenberg matrix obtained from Arnoldi iteration defined as

$$\mathbf{H} = \mathbf{V}^T \mathbf{J}_n \mathbf{V}. \tag{A.3}$$

The corresponding Krylov-subspace based approximation of the Jacobian is built as

$$\mathbf{A}_n = \mathbf{V} \mathbf{H} \mathbf{V}^T = \mathbf{V} \mathbf{V}^T \mathbf{J}_n \mathbf{V} \mathbf{V}^T. \tag{A.4}$$

The use of Krylov-subspace based approximation of the Jacobian reduces the φ and ψ function in accordance with lemma 4.2 and 4.3 to the following

$$\varphi_k(h \gamma \mathbf{A}_n) = \frac{1}{k!} (\mathbf{I} - \mathbf{V} \mathbf{V}^T) + \mathbf{V} \varphi_k(h \gamma \mathbf{H}) \mathbf{V}^T, \tag{A.5}$$

$$\psi_j(h \gamma \mathbf{A}_n) = \tilde{p}_j (\mathbf{I} - \mathbf{V} \mathbf{V}^T) + \mathbf{V} \psi_j(h \gamma \mathbf{H}) \mathbf{V}^T, \tag{A.6}$$

where \tilde{p}_j is defined as

$$\tilde{p}_j = \sum_{k=1}^j \frac{p_{j,k}}{k!}. \tag{A.7}$$

In order to derive the reduced stage formulation of the EPIRKK method we need to resolve the vectors in the formulation into components in the Krylov-subspace and orthogonal to it. Repeating the splittings from the main text:

- Splitting the internal stage vectors noting that $Y_0 \equiv y_n$:

$$Y_i = \mathbf{V} \lambda_i + Y_i^\perp \quad \text{where} \quad \mathbf{V}^T Y_i = \lambda_i, \quad (\mathbf{I} - \mathbf{V} \mathbf{V}^T) Y_i = Y_i^\perp. \tag{A.8}$$

- Splitting the right-hand side function evaluated at internal stage vectors while noting that $f_0 \equiv f(y_n)$:

$$f_i := f(Y_i) = \mathbf{V}\eta_i + f_i^\perp \quad \text{where} \quad \mathbf{V}^T f_i = \eta_i, \quad (\mathbf{I} - \mathbf{V}\mathbf{V}^T) f_i = f_i^\perp. \quad (\text{A.9})$$

- Splitting the non-linear Taylor remainder of the right-hand side functions:

$$\begin{aligned} r(Y_i) &= f(Y_i) - f(y_n) - \mathbf{A}_n(Y_i - y_n) = f_i - f_0 - \mathbf{V}\mathbf{H}\mathbf{V}^T(Y_i - y_n), \\ \text{where } \mathbf{V}^T r(Y_i) &= \eta_i - \eta_0 - \mathbf{H}(\lambda_i - \lambda_0), \\ (\mathbf{I} - \mathbf{V}\mathbf{V}^T) r(Y_i) &= f_i^\perp - f_0^\perp. \end{aligned} \quad (\text{A.10})$$

- Splitting the forward differences of the non-linear remainder terms:

$$\begin{aligned} \tilde{r}_{(j-1)} &:= \Delta^{(j-1)} r(y_n) = \mathbf{V} d_{(j-1)} + \tilde{r}_{(j-1)}^\perp, \\ \text{where } \mathbf{V}^T \tilde{r}_{(j-1)} &= d_{(j-1)}, \quad (\mathbf{I} - \mathbf{V}\mathbf{V}^T) \tilde{r}_{(j-1)} = \tilde{r}_{(j-1)}^\perp. \end{aligned} \quad (\text{A.11})$$

Using these each internal stage of the EPIRKK method can be expressed as below:

$$\begin{aligned} \mathbf{V}\lambda_i + Y_i^\perp &= y_n + h a_{i,1} \left(\tilde{p}_1 (\mathbf{I} - \mathbf{V}\mathbf{V}^T) + \mathbf{V} \psi_1(h g_{i,1} \mathbf{H}) \mathbf{V}^T \right) (\mathbf{V}\eta_0 + f_0^\perp) \\ &\quad + \sum_{j=2}^i h a_{i,j} \left(\tilde{p}_j (\mathbf{I} - \mathbf{V}\mathbf{V}^T) + \mathbf{V} \psi_j(h g_{i,j} \mathbf{H}) \mathbf{V}^T \right) (\mathbf{V} d_{(j-1)} + \tilde{r}_{(j-1)}^\perp) \\ &= y_n + h a_{i,1} \left(\tilde{p}_1 f_0^\perp + \mathbf{V} \psi_1(h g_{i,1} \mathbf{H}) \eta_0 \right) \\ &\quad + \sum_{j=2}^i h a_{i,j} \left(\tilde{p}_j \tilde{r}_{(j-1)}^\perp + \mathbf{V} \psi_j(h g_{i,j} \mathbf{H}) d_{(j-1)} \right). \end{aligned} \quad (\text{A.12})$$

The reduced stage formulation of the EPIRKK method is obtained by multiplying the above equation by \mathbf{V}^T from the left

$$\begin{aligned} \lambda_i &= \mathbf{V}^T y_n + h a_{i,1} \psi_1(h g_{i,1} \mathbf{H}) \eta_0 + \sum_{j=2}^i h a_{i,j} \psi_j(h g_{i,j} \mathbf{H}) d_{(j-1)} \\ &= \lambda_0 + h a_{i,1} \psi_1(h g_{i,1} \mathbf{H}) \eta_0 + \sum_{j=2}^i h a_{i,j} \psi_j(h g_{i,j} \mathbf{H}) d_{(j-1)}. \end{aligned} \quad (\text{A.13})$$

And the full stage vector can be recovered by first computing the reduced stage vector and adding the orthogonal piece Y_i^\perp obtained when multiplying equation (A.12) by $(\mathbf{I} - \mathbf{V}\mathbf{V}^T)$

$$\begin{aligned} Y_i^\perp &= (\mathbf{I} - \mathbf{V}\mathbf{V}^T) y_n + h a_{i,1} \tilde{p}_1 f_0^\perp + \sum_{j=2}^i h a_{i,j} \tilde{p}_j \tilde{r}_{(j-1)}^\perp \\ &= (y_n - \mathbf{V}\lambda_0) + h a_{i,1} \tilde{p}_1 f_0^\perp + \sum_{j=2}^i h a_{i,j} \tilde{p}_j \tilde{r}_{(j-1)}^\perp. \end{aligned} \quad (\text{A.14})$$

The final stage can also be written in the above form with multipliers b_i in place of a_{ij} . Notice that the expensive computations are performed in the reduced space, i.e. the ψ function is computed in the reduced space instead of the full space offering potential computational savings. In the above equations, the

quantities $d_{(j-1)}$ and $\tilde{r}_{(j-1)}^\perp$ can be shown to be

$$d_{(j-1)} = \sum_{k=0}^{j-1} \left((-1)^k \binom{j-1}{k} \eta_{j-1-k} - \mathbf{H} \left((-1)^k \binom{j-1}{k} \lambda_{j-1-k} \right) \right), \quad (\text{A.15})$$

$$\tilde{r}_{(j-1)}^\perp = \sum_{k=0}^{j-1} \left((-1)^k \binom{j-1}{k} f_{j-1-k}^\perp \right), \quad (\text{A.16})$$

as is done in the following appendix.

B. Proofs

In order to prove equations (23a) and (23b), we start with the definition of the remainder function and forward difference.

$$r(y) = f(y) - f(y_n) - \mathbf{A}_n(y - y_n), \quad (\text{B.1})$$

$$\Delta^{(j)} r(Y_i) = \Delta^{(j-1)} r(Y_{i+1}) - \Delta^{(j-1)} r(Y_i), \quad (\text{B.2a})$$

$$\Delta^{(1)} r(Y_i) = r(Y_{i+1}) - r(Y_i). \quad (\text{B.2b})$$

Lemma B.1. $\Delta^{(j)} r(Y_i) = \sum_{k=0}^j (-1)^k \binom{j}{k} r(Y_{i+j-k})$.

Proof. In order to prove the lemma, we resort to mathematical induction. Base case $j = 1$,

$$\begin{aligned} \Delta^{(1)} r(Y_i) &= \sum_{k=0}^1 (-1)^k \binom{1}{k} r(Y_{i+1-k}) \\ &= r(Y_{i+1}) - r(Y_i). \end{aligned}$$

The base case is true by definition. We now assume that the proposition holds true for all j up to $k-1$. We have,

$$\Delta^{(k-1)} r(Y_i) = \sum_{l=0}^{k-1} (-1)^l \binom{k-1}{l} r(Y_{i+k-1-l}), \quad (\text{B.3})$$

$$\Delta^{(k-1)} r(Y_{i+1}) = \sum_{l=0}^{k-1} (-1)^l \binom{k-1}{l} r(Y_{i+k-l}). \quad (\text{B.4})$$

Then for $j = k$,

$$\begin{aligned} \Delta^{(k)} r(Y_i) &= \Delta^{(k-1)} r(Y_{i+1}) - \Delta^{(k-1)} r(Y_i) \\ &= \sum_{l=0}^{k-1} (-1)^l \binom{k-1}{l} r(Y_{i+k-l}) - \sum_{l=0}^{k-1} (-1)^l \binom{k-1}{l} r(Y_{i+k-1-l}) \\ &= r(Y_{i+k}) + \sum_{l=1}^{k-1} (-1)^l \binom{k-1}{l} r(Y_{i+k-l}) - \sum_{l=0}^{k-2} (-1)^l \binom{k-1}{l} r(Y_{i+k-1-l}) + (-1)^k r(Y_i). \end{aligned}$$

We perform a change of variable for the second summation, $m = l + 1 \implies l = (m - 1)$,

$$\begin{aligned}
\Delta^{(k)}r(Y_i) &= r(Y_{i+k}) + \sum_{l=1}^{k-1} (-1)^l \binom{k-1}{l} r(Y_{i+k-l}) - \sum_{m=1}^{k-1} (-1)^{m-1} \binom{k-1}{m-1} r(Y_{i+k-m}) + (-1)^k r(Y_i) \\
&= r(Y_{i+k}) + \sum_{l=1}^{k-1} (-1)^l \binom{k-1}{l} r(Y_{i+k-l}) + \sum_{m=1}^{k-1} (-1)^m \binom{k-1}{m-1} r(Y_{i+k-m}) + (-1)^k r(Y_i).
\end{aligned}$$

The summations run between the same start and end indices, and can be collapsed.

$$\Delta^{(k)}r(Y_i) = r(Y_{i+k}) + \sum_{l=1}^{k-1} (-1)^l \left(\binom{k-1}{l} + \binom{k-1}{l-1} \right) r(Y_{i+k-l}) + (-1)^k r(Y_i).$$

We use the identity,

$$\binom{k-1}{l} + \binom{k-1}{l-1} = \binom{k}{l},$$

and arrive at the desired result,

$$\begin{aligned}
\Delta^{(k)}r(Y_i) &= r(Y_{i+k}) + \sum_{l=1}^{k-1} (-1)^l \binom{k}{l} r(Y_{i+k-l}) + (-1)^k r(Y_i) \\
&= (-1)^0 \binom{k}{0} r(Y_{i+k}) + \sum_{l=1}^{k-1} (-1)^l \binom{k}{l} r(Y_{i+k-l}) + (-1)^k \binom{k}{k} r(Y_i) \\
&= \sum_{l=0}^k (-1)^l \binom{k}{l} r(Y_{i+k-l}).
\end{aligned} \tag{B.5}$$

□

Lemma B.2. *Given*

$$\Delta^{(j-1)}r(y_n) = \mathbf{V}d_{(j-1)} + \tilde{r}_{(j-1)}^\perp, \tag{B.6}$$

we need to prove

$$d_{(j-1)} = \sum_{k=0}^{j-1} \left((-1)^k \binom{j-1}{k} \eta_{j-1-k} - \mathbf{H} \left((-1)^k \binom{j-1}{k} \lambda_{j-1-k} \right) \right), \tag{B.7}$$

$$\tilde{r}_{(j-1)}^\perp = \sum_{k=0}^{j-1} \left((-1)^k \binom{j-1}{k} f_{j-1-k}^\perp \right). \tag{B.8}$$

Proof. We start with lemma B.1 where we have proven that

$$\Delta^{(j)}r(Y_i) = \sum_{k=0}^j (-1)^k \binom{j}{k} r(Y_{i+j-k}).$$

We plugin the value $i = 0$ which corresponds to $\Delta^{(j)}r(Y_0) \equiv \Delta^{(j)}r(y_n)$ and we get,

$$\Delta^{(j)}r(y_n) = \sum_{k=0}^j (-1)^k \binom{j}{k} r(Y_{j-k}).$$

WLOG replacing j by $j - 1$ yields

$$\Delta^{(j-1)}r(y_n) = \sum_{k=0}^{j-1} (-1)^k \binom{j-1}{k} r(Y_{j-1-k}). \quad (\text{B.9})$$

Since the left-hand side of equation (B.9) can be written as

$$\Delta^{(j-1)}r(y_n) = \mathbf{V}d_{(j-1)} + \tilde{r}_{(j-1)}^\perp,$$

we have the following result

$$\mathbf{V}d_{(j-1)} + \tilde{r}_{(j-1)}^\perp = \sum_{k=0}^{j-1} (-1)^k \binom{j-1}{k} r(Y_{j-1-k}). \quad (\text{B.10})$$

The remainder function $r(Y_i)$ is defined as

$$r(Y_i) = f(Y_i) - f(y_n) - \mathbf{A}_n * (Y_i - y_n).$$

Plugging in the definition of remainder function in (B.10) and observing that $r(y_n) = 0$, we get

$$\begin{aligned} \mathbf{V}d_{(j-1)} + \tilde{r}_{(j-1)}^\perp &= \sum_{k=0}^{j-2} (-1)^k \binom{j-1}{k} \left(f(Y_{j-1-k}) - f(y_n) - \mathbf{A}_n * (Y_{j-1-k} - y_n) \right) \\ &= \sum_{k=0}^{j-2} (-1)^k \binom{j-1}{k} \left(f(Y_{j-1-k}) - \mathbf{A}_n * Y_{j-1-k} \right) - \\ &\quad \sum_{k=0}^{j-2} (-1)^k \binom{j-1}{k} \left(f(y_n) - \mathbf{A}_n * y_n \right). \end{aligned} \quad (\text{B.11})$$

Consider the identity involving alternating sum and difference of binomial coefficients,

$$\sum_{i=0}^k (-1)^i \binom{k}{i} = 0. \quad (\text{B.12})$$

Applying (B.12) to (B.11) we get,

$$\begin{aligned} \mathbf{V}d_{(j-1)} + \tilde{r}_{(j-1)}^\perp &= \sum_{k=0}^{j-2} (-1)^k \binom{j-1}{k} \left(f(Y_{j-1-k}) - f(y_n) - \mathbf{A}_n * (Y_{j-1-k} - y_n) \right) \\ &= \sum_{k=0}^{j-2} (-1)^k \binom{j-1}{k} \left(f(Y_{j-1-k}) - \mathbf{A}_n * Y_{j-1-k} \right) - \\ &\quad (-1)^{(j-1)} \left(f(y_n) - \mathbf{A}_n * y_n \right) \\ &= \sum_{k=0}^{j-2} (-1)^k \binom{j-1}{k} \left(f(Y_{j-1-k}) - \mathbf{A}_n * Y_{j-1-k} \right) + \\ &\quad (-1)^{(j-1)} \binom{j-1}{j-1} \left(f(y_n) - \mathbf{A}_n * y_n \right) \\ &= \sum_{k=0}^{j-1} (-1)^k \binom{j-1}{k} \left(f(Y_{j-1-k}) - \mathbf{A}_n * Y_{j-1-k} \right). \end{aligned} \quad (\text{B.13})$$

Additionally, since we are replacing the Jacobian by the approximation in the Krylov-subspace, i.e. $\mathbf{A}_n = \mathbf{V}\mathbf{H}\mathbf{V}^T$ we have

$$\mathbf{V}d_{(j-1)} + \tilde{r}_{(j-1)}^\perp = \sum_{k=0}^{j-1} (-1)^k \binom{j-1}{k} \left(f(Y_{j-1-k}) - \mathbf{V}\mathbf{H}\mathbf{V}^T * Y_{j-1-k} \right). \quad (\text{B.14})$$

We get the expression for $d_{(j-1)}$ by multiplying equation (B.14) from the left by V^T and that for $\tilde{r}_{(j-1)}^\perp$ by multiplying by $(\mathbf{I} - \mathbf{V}\mathbf{V}^T)$. □

C. Structure of Jacobian evaluated at y_0 for the test problems

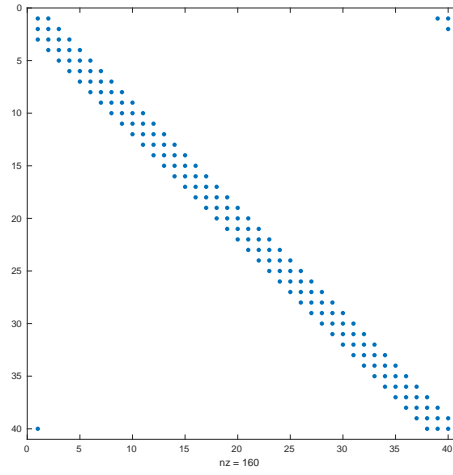


Figure C.13: Structure of Jacobian evaluated at y_0 for the Lorenz-96 system (30)

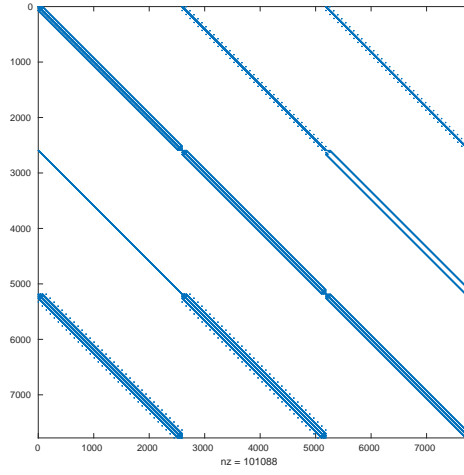


Figure C.14: Structure of Jacobian evaluated at y_0 for the Shallow Water Equations (31)

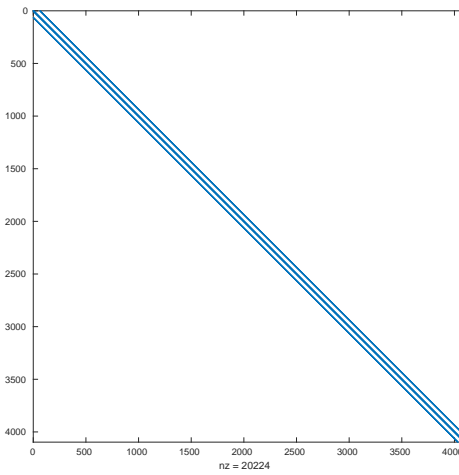


Figure C.15: Structure of Jacobian evaluated at y_0 for the Allen-Cahn Equations (32) on a 64×64 grid.

References

References

- [1] Samuel M. Allen and John W. Cahn. A microscopic theory for antiphase boundary motion and its application to antiphase domain coarsening. *Acta Metallurgica*, 27(6):1085 – 1095, 1979.
- [2] A. Augustine and A. Sandu. MATLODE: A MATLAB ODE solver and sensitivity analysis toolbox. *ACM TOMS*, in preparation, 2018.
- [3] J.C. Butcher. *Numerical methods for ordinary differential equations*. John Wiley & Sons, Ltd, 2nd edition, 2008.
- [4] J.C. Butcher. Trees, B-series and exponential integrators. *IMA Journal of Numerical Analysis*, 30:131–140, 2010.
- [5] D. N. Daescu and I. M. Navon. Adaptive observations in the context of 4D-Var data assimilation. *Meteorology and Atmospheric Physics*, 85(4):205–226, 2004.
- [6] E. Hairer, S.P. Norsett, and G. Wanner. *Solving ordinary differential equations I: Nonstiff problems*. Number 8 in Springer Series in Computational Mathematics. Springer-Verlag Berlin Heidelberg, 1993.
- [7] E. Hairer and G. Wanner. *Solving ordinary differential equations II: Stiff and differential-algebraic problems*. Number 14 in Springer Series in Computational Mathematics. Springer-Verlag Berlin Heidelberg, 2 edition, 1996.
- [8] M. Hochbruck and C. Lubich. On Krylov subspace approximations to the matrix exponential operator. *SIAM Journal on Numerical Analysis*, 34(5):1911–1925, 1997.
- [9] M. Hochbruck, C. Lubich, and H. Selhofer. Exponential integrators for large systems of differential equations. *SIAM Journal on Scientific Computing*, 19(5):1552–1574, 1998.
- [10] M. Hochbruck and A. Ostermann. Exponential integrators. *Acta Numerica*, 19:209–286, 2012.
- [11] M. Hochbruck, A. Ostermann, and J. Schweitzer. Exponential Rosenbrock-type methods. *SIAM Journal on Numerical Analysis*, 47:786–803, 2009.
- [12] Edward N. Lorenz. Predictability – a problem partly solved. In Tim Palmer and Renate Hagedorn, editors, *Predictability of Weather and Climate*, pages 40–58. Cambridge University Press (CUP), 1996.
- [13] B Neta, FX Giraldo, and IM Navon. Analysis of the Turkel–Zwas scheme for the two-dimensional shallow water equations in spherical coordinates. *Journal of Computational Physics*, 133(1):102–112, 1997.
- [14] Jitse Niesen and Will M. Wright. Algorithm 919: A krylov subspace algorithm for evaluating the e^A -functions appearing in exponential integrators. *ACM Trans. Math. Softw.*, 38(3):22:1–22:19, April 2012.
- [15] G. Rainwater and M. Tokman. A new approach to constructing efficient stiffly accurate epirk methods. *Journal of Computational Physics*, 323:283 – 309, 2016.
- [16] Vishwas Rao and Adrian Sandu. A posteriori error estimates for the solution of variational inverse problems. *SIAM/ASA Journal on Uncertainty Quantification*, 3(1):737–761, 2015.
- [17] J. C. Schulze, P. J. Schmid, and J. L. Sesterhenn. Exponential time integration using krylov subspaces. *International Journal for Numerical Methods in Fluids*, 60(6):561–609, 2008.
- [18] Roger B. Sidje. Expokit: a software package for computing matrix exponentials. *ACM Transactions on Mathematical Software*, 24(1):130–156, mar 1998.
- [19] Trond Steihaug and Arne Wolfbrandt. An attempt to avoid exact Jacobian and nonlinear equations in the numerical solution of stiff differential equations. *Mathematics of Computation*, 33(146):521–521, may 1979.
- [20] M. Tokman. Efficient integration of large stiff systems of ODEs with exponential propagation iterative (EPI) methods. *Journal of Computational Physics*, 213(2):748–776, 2006.
- [21] M. Tokman. A new class of exponential propagation iterative methods of Runge–Kutta type (EPIRK). *Journal of Computational Physics*, 230:8762–8778, 2011.
- [22] Mayya Tokman and John Loffeld. Efficient design of exponential-krylov integrators for large scale computing. *Procedia Computer Science*, 1(1):229–237, 2010.
- [23] Mayya Tokman, John Loffeld, and Paul Tranquilli. New adaptive exponential propagation iterative methods of runge–kutta type. *SIAM Journal on Scientific Computing*, 34(5):A2650–A2669, 2012.
- [24] Paul Tranquilli, S. Ross Glandon, Arash Sarshar, and Adrian Sandu. Analytical Jacobian-vector products for the matrix-free time integration of partial differential equations. *Journal of Computational and Applied Mathematics*, 2016.
- [25] Paul Tranquilli and Adrian Sandu. Exponential–Krylov methods for ordinary differential equations. *Journal of Computational Physics*, 278(0):31 – 46, 2014.
- [26] Paul Tranquilli and Adrian Sandu. Rosenbrock–Krylov methods for large systems of differential equations. *SIAM Journal on Scientific Computing*, 36(3):A1313–A1338, 2014.
- [27] Henk A. van der Vorst. *Iterative Krylov methods for large linear systems*. Cambridge University Press, 2003.